Environmental Research Center Papers

NUMBER 5

1984

Environmental Research Center
The University of Tsukuba

AN EXPERIMENTAL STUDY OF DUNE DEVELOPMENT AND ITS EFFECT ON SEDIMENT SUSPENSION*

By Fujiko Iseya**

(received February 23, 1984)

ABSTRACT

In alluvial sand-bed rivers, it is found that the concentration of suspended bed material load (referred to as the "suspended sediment" in this paper) is higher during the rising stage than during the falling stage of a flood, in which the water discharge changes rapidly enough. In this study, the mechanism of this phenomenon was examined in a large sand-bed recirculating flume. The flume tests, which were designed to evaluate a possible relation between the sediment suspension and the bedform, were performed under such hydraulic conditions that dunes in the lower flow regime developed.

Run simulating a runoff event indicated that the suspended sediment concentration was extremely high during the rising leg of a flood hydrograph, when the dune grew. Six different runs with constant discharge revealed that changes in the bed configuration could be classified into two stages. One is "Developing dune stage" and the other is "Equilibrium dune stage". It is concluded from continual measurements of suspended sediment that suspended sediment concentration is higher in the developing dune stage than in the equilibrium dune stage. In the developing dune stage, strong eddies associated with the dune growth carry large amount of sediment particles periodically from the bed surface into the main flow. On the other hand, in the equilibrium dune stage, suspended sediment concentration has little variation with time, because only weak eddies are generated in spite of the presence of largest dunes on the bed surface. The examination on the time required to attain the equilibrium dune size makes it clear that the larger the stream power is, the longer time it takes to attain the equilibrium dune size.

During floods of natural rivers, the stream power at a station increases as the water discharge increases. Therefore, it is reasonable to state that the developing dune stage is always present in the rising rimb of a runoff event in which the water discharge changes rapidly. The active growth of dune dimensions in the rising stage of a flood has a notable effect on turbulant flow and thus on sediment suspension. It can be concluded that the high suspended sediment concentration in the rising leg of a flood hydrograph is strongly affected by the rapid growth of dunes.

---

*A dissertation submitted in partial fulfillment of the requirements for the degree of Doctor of Science in Doctoral Program in the University of Tsukuba

**Address from April 1, 1984 is the Environmental Research Center, the University of Tsukuba, Ibaraki 305 Japan

CONTENTS

LIST OF FIGURES

LIST OF TABLES

CHAPTER I

INTRODUCTION

1-1 Previous studies on suspended load in natural rivers

Total load transported by the fluid flow in natural rivers may be distinguished either by source or by transporting mechanism as shown in Table 1. Suspended load is a terminology according to the transporting mechanism and is defined as the sediment particles moving outside the bed layer (Einstein, 1950).

Table 1 Classification of sediment transport in alluvial river channels. Modified after Lewin (1981, p. 201)

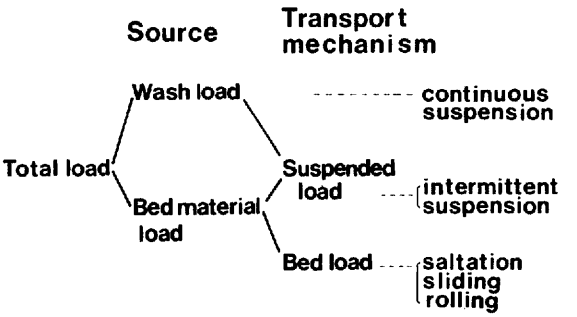

Suspended load is usually divided into two components, while both components are simultaneously sampled in hydrological measurements in natural rivers. One is the finest sediment derived from supply sources to the actual channel. Such fine material is held almost continously in suspension. The other is the coarser sediment derived from the bed material itself. Such coarse material is intermittently taken into suspension by the turbulent flow. The former is the so-called "wash load" and the latter is called "suspended bed material load" by Shen (1971a), Richard (1982, p.96), and Lewin (1983), or "intermittent suspension load" by Middleton & Southard (1977).

Intensive sampling programs have been carried out in various streams and these hydrological investigations show that the relationship between suspended load concentration and water discharge is usually plotted as a straight line on logarithmic coordinates (Straub, 1932; Leopold & Maddock, 1953; Graf, 1971, p.235-237). This indicates that an increase in stream discharge is accompanied by an increase in suspended load concentration.

However, such rating plot often reveals considerable scatter about the straight line relationship. Studies by Guy (1964), Hall (1967), and Walling & Teed (1971) have demonstrated that suspended sediment concentrations are generally greater in summer than in winter and thus the seasonal effects are often important.

A further important cause of rating plot scatter is that the peak of suspended load concentration rarely coincides with the peak of a flood hydrograph. The maximum concentration of suspended load generally precedes the peak water discharge (Leopold & Maddock, 1953; Kikkawa, 1954; Nordin, 1964; Guy, 1964; Nordin & Beverage, 1965; Walling & Teed, 1971; Graf, 1971,

p.235-237; Wood, 1977). For example, Nordin (1964) plotted sediment concentration which contained both fine material and sand-size material against daily mean water discharge during the period from April to July in 1958 in the Rio Grande near Bernalillo, New Mexico and showed that the maximum concentration preceded the maximum discharge by a period of about six weeks.

On some rivers, however, the peak of suspended load concentration can be significantly behind the flood peak. Heidel (1956) concluded from his extensive measurements at four different stations of the Bighorn River in Montana and Wyoming that the peak of suspended load concentration occurred after the peak of water discharge with a progressive lag.

Gregory & Walling (1973, p. 217-218) and Richard (1982, p. 104-105) stated that hysteresis in the change of suspended load concentration through a single storm, in which the maximum sediment concentration may occur either in advance or behind the peak of water discharge, reflects two main influences. One is the sediment supply changes between the rising and falling flood stages, in which the change of wash load concentration during a storm runoff plays an important role in the sediment concentration vs. water discharge relation. As fine material on the land surface is washed into the stream within a short period, the maximum sediment production or availability usually occurs in the early stages of a storm event. The other influence is the spatial effect of a storm size relative to a catchment area and the associated lag effect of the downstream travel of sediment and water 'waves'. Heidel (1956) established that the sediment concentration peak moved more slowly than the water discharge peak and that the sediment peak progressively lagged behind the flood peak in a downstream direction.

1-2 Problems and the purpose of this study

It has been an ultimate objective for hydraulic engineers to accurately predict the rate of sediment transport for all flow conditions in alluvial river channels. In order to pursue this objective, it is necessary to separate the suspended load into the suspended bed material load (referred to as "suspended sediment" in this paper) and the wash load, and to analyze them respectively. Because the amount of wash load does not depend on the hydraulic conditions but on the supply rate (Einstein et al. 1940; Shen, 1971a), and thus a satisfactory prediction of wash load concentration based on hydraulic properties of the channel flow is extremely difficult at the moment.

In this paper, attention is focused on the relationship between suspended sediment and flow conditiodns in a channel. From the previous hydrological studies described above, the knowledge on (1) the contribution of suspended sediment to the entire suspended load and (2) the change of suspended sediment concentration during a runoff event has not fully obtained. Because suspended sediment and wash load were simultaneously sampled as "suspended load" and they were not separatedly discussed in the field studies.

In reality, there is probably no sharp distinction between two components of suspended load. However, the component of silt-clay size (< 0.063 mm) is conventionally considered to be the wash load, and the sand size component (> 0.063 mm) is considered to be the suspended sediment (Richard, 1982, p. 99). As a rule of thumb, many engineers also assume the grain size of wash load to be smaller than 0.063 mm (Shen, 1971b). This arbitrary criterion between suspended sediment and wash load is based on a fact that the vertical concentration-gradient is commonly uniform for the silt-clay size fraction, but that the gradient is steeply decreasing with height above the bed for the sand size fraction. This was confirmed in many rivers such as the middle Rio Grande, New

Mexico (Nordin & Dempster, 1963), the Mississippi River at St. Louis, Missouri (Scott & Stephens, 1966), and the Sakura River, Ibaraki Prefecture, Japan (Iseya, 1979).

Based on this arbitrary criterion, Iseya (1982a) studied the detailed shape of suspended sediment vs. flood stage graph for individual storm event in the Sakura River and showed that the peak of suspended sediment discharge occurred in the rising stage of a flood (Fig. 1). Moreover, the observational result of Kinoshita (1982) in the lower Tone River, one of the largest rivers in Japan, also indicates that the maximum concentration of suspended sediment near the water surface during a typhoon-caused large flood preceded the maximum discharge by a period of about five to eight hours.

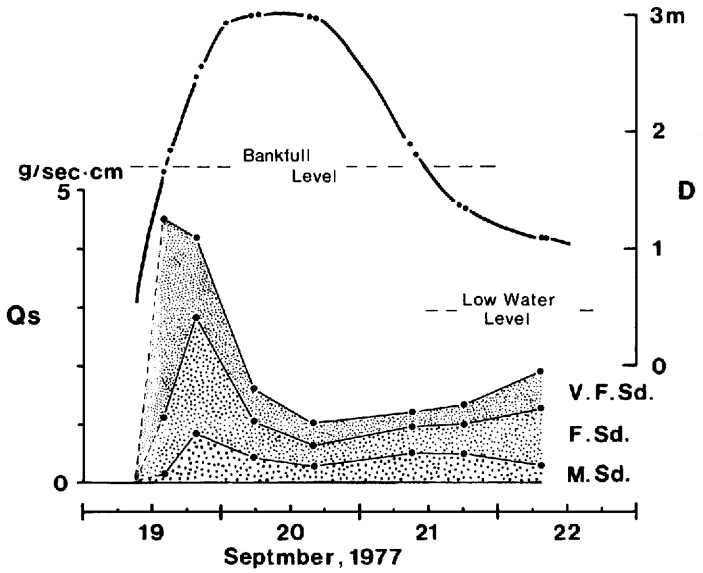

Fig. 1 Variation of suspended sediment discharge in the Sakura River, Ibaraki Prefecture, Japan (Iseya, 1982a).
Q_S : suspended sediment discharge
D : water depth
V. F. Sd. : very fine sand, 0.063–0.125 mm
F. Sd. : fine sand, 0.125–0.25 mm
M. Sd. : medium sand, 0.25–0.5 mm

These two examples are contradictory to theoretical treatments between suspended sediment concentration and flow intensity. Theoretically, the transport of suspended sediment is controlled by the tractive force of stream (Lane & Kalinske, 1941; Einstein, 1950). This means that there is a close single relationship between the suspended sediment and water discharge.

It has been also recognized that suspension of sandy bed material is strongly influenced by water temperature (Vanoni, 1975, p. 72-78; Richard, 1982, p. 104). Since the higher viscosity at low water temperature reduces the fall velocity and hence the effective sediment size, a decrease in temperature causes an increase in sediment transport. Especially in the case of a snow melt flood continuing for some months, the change of water temperature would have more notable effect on sediment suspension. But this factor may not contribute to the change of suspended sediment concentration during a short period flood in which the water temperature does not so

much change.

In laboratory flumes, it has been emphasized that the vertical velocity-gradient becomes steeper and the traction force near the bed increases as the wash load concentration increases (for example, Vanoni, 1944; Kikkawa & Fukuoka, 1968). Nordin & Dempster's (1963) observation in the middle Rio Grande, New Mexico indicated that the fall velocity was effectively decreased in flows with high suspended load concentration greater than about 10,000 ppm. It can be expected that concentration of suspended sediment will be increased by the high wash load concentration.

However, these give no reasonable explanation on the cause of the discrepancy of peaks between suspended sediment concentration and water discharge. Namely, sediment data obtained in the Futagami River, a tributary of the Sakura River (Iseya, 1982b, Fig. 2), also showed that the maximum concentration of suspended sediment preceded a flood peak, nevertheless the highest wash load concentration of 7,550 ppm occurred when water level declined.

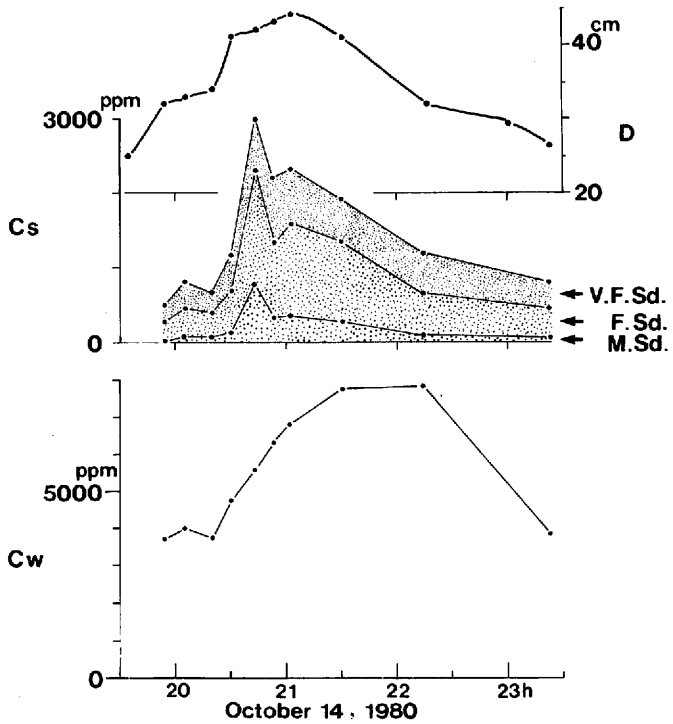

Fig. 2 Variation of suspended load concentration on the water surface in the Futagami River, a tributary of the Sakura River, Ibaraki Prefecture, Japan (Iseya, 1982b).
C_S : concentration of suspended sediment (sand)
C_W : concentration of wash load (silt–clay)
D : water depth
V. F. Sd. : very fine sand, 0.063–0.125 mm
F. Sd. : fine sand, 0.125–0.25 mm
M. Sd. : medium sand, 0.25–0.5 mm

In short, existing theoretical and empirical studies on the suspended sediment concentration give no suitable explanations to the problem why the maximum concentration of suspended sediment occurs during the rising stage of a runoff event. The purpose of this study is to tackle this problem, and flume experiments were carried out to accomplish this purpose.

In such rivers as shown in Figs. 1 and 2, a runoff event is characterized by a marked change in water discharge in a short period of time. It can be expected that a continuous feedback system among sediment transport, bedforms and turbulent flows is much stronger at work under such unsteady flow conditions as compared with steady conditions. Therefore, it is a clearly inadequate approach to try to investigate one portion in isolation. The flume tests in this study were specially designed to investigate the behavior of bedforms and the changes of flow characteristics as well as the change of suspended sediment transport under varying flow conditions.

CHAPTER II

EQUIPMENT AND PROCEDURE

2-1 Flume and bed material

The experiments were conducted in a large recirculating flume, which is 4 m wide, 160 m long and 2 m deep, at the Environmental Research Center of the University of Tsukuba (Fig. 3). Detailed descriptions on the facility are given by Inokuchi et al. (1980) and Ikeda (1983).

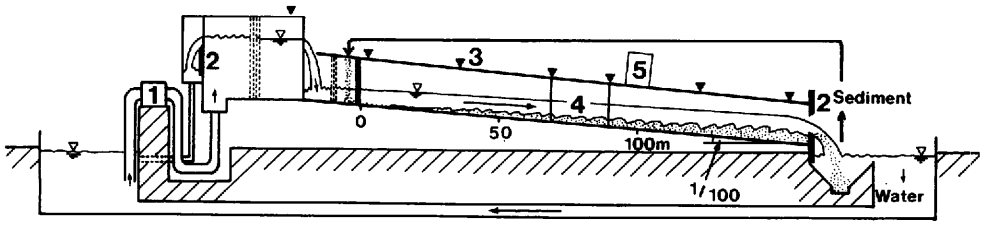

Fig. 3 Schematic diagram of the 4-meter-wide flume used in the study.
1: pumps, 2: gate. 3: electric water level meter, 4: transparent viewing window, 5: measuring carriage

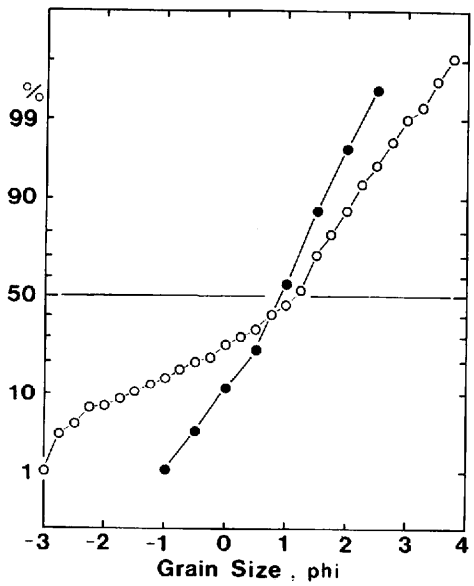

Fig. 4 Grain size distribution of bed material used in the study. Values expressed by solid circles were determined by using the settling tube system modified after Gibbs (1971). Values obtained from ten samples were averaged in order to eliminate the scatter among samples. Values expressed by open circles were determined by using sieves.

The flume is made of steel and the bottom is fixed at a slope of 1/100. However, the inclination of the bed surface can be varied from a slope of 0 to 1/50 by operating a tailgate at the end of the flume. Water discharge is regulated by three pumps and by the operation of a gate in the high water tank to a maximum of approximately 1.5 m^3/sec. A desired discharge can be readily adjusted and kept constant for many hours. Gradual increase or decrease of water discharge can be also controlled.

Both side walls of the flume have 20-m long transparent Plexiglas sections midway to allow observations of sediment movement and of sedimentary structures of dunes. A carriage which can be moved by an electric motor along rails mounted on both walls is used for the measurement.

The bed material used in the experiments is poorly sorted sand excavated from the bottom of the Lake Kasumiga-Ura, Ibaraki Prefecture (Fig. 4). This material has a median fall diameter of 0.57 mm and contains approximately 41% medium sand and 45% coarse sand.

2-2 Experimental condition and procedure

The experiments were carried out under such hydraulic conditions that dunes in the lower flow regime developed on an initially flat bed. Two cases of experiments were conducted: Case 1 constitutes a run with varying water discharge, and Case 2 has six runs in which the water discharge was held constant.

The procedure of each run is as follows:

(1) A desired bed slope was set and the sand surface was smoothed along the flume.
(2) Water was introduced into the flume. Sediment and hydraulic data acquisition started just after commencement of a run.
(3) After allowing water to flow for a given time, the run was interrupted to measure the bedform. The flume had been filled with water by closing a tailgate in the downstream end before the pumps were stopped. Backwater effect could eliminate the disturbance of bedform; this disturbance was expected to occur by the interruption of run.
(4) Longitudinal profiles of the bed surface were measured using a sonic sounder.
(5) The flume was then slowly drained.
(6) Photographs of the bed surface were taken.
(7) The flume was gently filled with water to the desired still water level again to save the bedform from the disturbance caused by stop-start sequence. The water was introduced at the lower end of the flume.
(8) The pumps were started again. The water surface slope was gradually increased by adjusting the tailgate to make it parallel to the bed slope.

The above procedure from (2) to (8) was repeated in one run. Each repetition is referred to as the "Step" in this paper.

2-3 Measurement of variables

In the present experimental program, the following three kinds of variables were especially measured.

1. Suspended sediment concentration

A sampling point was fixed at the center of the flume (2 m from the side walls) and at a distance of 85 m from the flume inlet.

Sediment-water samples were collected every 1 to 15 min throughout each run. It was possible

to simultaneously collect suspended sediment samples at three different depths by using a set of three siphon nozzles. The sampler was attached to the end of a small transverse carriage equipped on the main carriage (Fig. 5). Each nozzle had an inner opening of 13 mm. Intake velocity at the sampler nozzle was made equal to the average flow velocity by controlling a valve at the outlet of siphon tube. It took about one minute or more to obtain an 8–10 liter sediment-water sample from each depth.

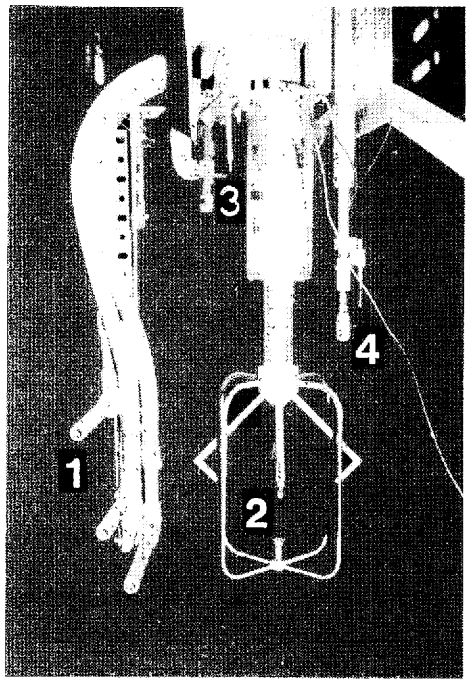

Fig. 5 Measuring devices.
1: a set of three siphone nozzles, 2: sonic current meter, 3: water level meter, 4: sand level gauge

The sediment-water sample was divided into the sand size material and the water containing the silt-clay size material by using a 4-phi (0.063 mm) sieve. Suspended sediment concentration was calculated after the sand size material was dried and weighed. The grain size distribution of suspended sediment was analyzed by using a settling tube system modified after Gibbs (1971).

Some of the water samples were decanted off after the silt-clay was settled. The residues were then thoroughly dried and weighed to calculate the silt-clay concentration or the wash load concentration. Because the wash load concentration had little variation during a run, the average value of some samples was calculated.

2. Bedform

–Dune length and height–

Measurement of the bedform was made along 40 m to 110 m from flume inlet. A pair of longitudinal profiles of the bed surface along two lines, each located about one-third of the width from both walls, was measured using a sonic sounder. Data on dune length and height were based

on these profiles.

–Dune velocity–

The speed of dune migration was obtained from successive measurements of the position of dune brinkpoint through the Plexiglas wall of the flume.

–Plan form of dunes–

Photographs were taken during each run after carefull draining.

3. Flow characteristics

The surface velocity of the flow was measured by using floats. The flow patterns on the water surface were visually observed and photographed. Flow characteristics over dunes were also observed through the Plexiglas wall of the flume.

Fluctuating velocity components at the sediment-water sampling point were measured with a three-dimensional sonic current meter (Kaijo Denki Model FC current meter, Fig. 5). Each sensing head has a sound path of 7.5 cm. Analog signals from the current meter were picked up 10 times a second, and they were digitized and recorded on magnetic tapes. The signals were also continuously monitored by a chart recorder. A computer program was developed to calculate turbulent statistics. The methods of data collection and analysis were basically given by Kai (1982).

The basic hydraulic data were collected as follows. Results are tabulated in Tables 3 through 8.

1. Water discharge

Water discharge was measured by a triangular weir in a head tank. The elevation of water surface in the tank was continuously measured by an electric water-level meter.

2. Water surface slope

Elevations of the water surface were continuously recorded at six points along the flume by using electric water-level meters (Fig. 3). The average elevation of each point was used to calculate a mean water surface slope.

3. Water depth

Mean water depth was determined by measuring the difference in the elevation between the water surface and the bed surface. The measurement was made at the sediment-water sampling point.

As the water surface was subjected to rhythmic fluctuations, the water level was continuously measured and recorded by the electric water-level meter. The bed surface elevation at the fixed point also fluctuated owing to the dune migration. Bed surface elevation was measured every 10 sec by using an electric sand level gauge (Fig. 5). Mean bed elevation, however, was assumed to be equal to the initial bed elevation when the mean water depth was calculated. The incomings and outgoings of the bed material were balanced in the entire flume system, because the sediment carried by the sediment recirculating system from the downstream end of the flume was fed into the upstream end.

4. Water temperature

The water temperature was measured with a thermometer. An average of 2 to 5 readings was used as the water temperature at the time.

5. Additional hydraulic parameters

Additional hydraulic parameters such as Froude number and stream power were calculated from the above basic data.

CHAPTER III

EXPERIMENTAL RESULTS

3-1 Run with varying discharge (Case 1)

Case 1 is a run simulating a runoff event. The discharge was changed smoothly from the minimum of 0.4 m^3/sec to the maximum of 1.53 m^3/sec as indicated in Fig. 6. The resultant time-discharge curve resembles time-discharge relations of natural rivers.

The bed slope was fixed about 1/400. Because no tailgate control was made during the run, the water surface slope varied with discharge (Fig. 6). Such variation is also observed in natural channels.

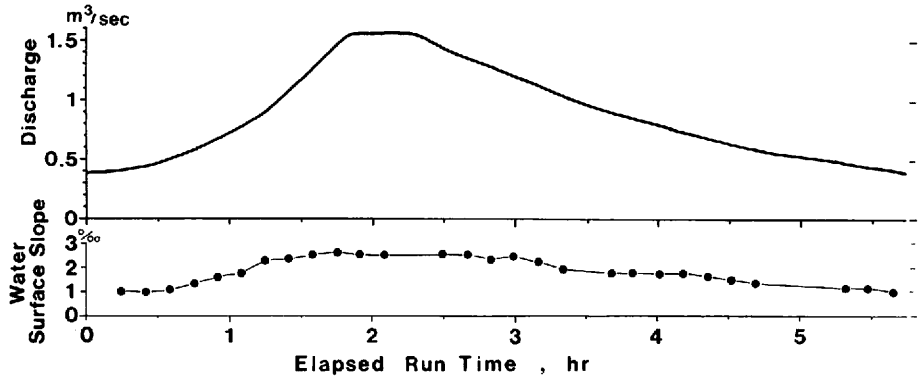

Fig. 6 Changes of water discharge and water surface slope in Case 1.

3-1-1 Variation of suspended sediment concentration

The experiment confirmed that the suspended sediment concentrations are higher during the rising stage than during the falling stage of a flood and that the highest concentration of suspended sediment precedes the peak discharge. Figure 7-2 shows the temporal variation of suspended sediment concentration at three different depths. The lack of data from the lowest sampling tube was caused by clogging of the nozzle. Because the lowest sampling nozzle was set near the bed surface, the nozzle was clogged up with the bed material when some of dune crests passed through the sampling point. Long time was needed to take the material off from the nozzle to resume sampling.

Figure 7-2 clearly shows that the high suspended sediment concentrations at each depth occurred from 1 to 2 hours after the beginning of the run. The comparison of Figs. 7-1 and 7-2 indicates that it is during the rising stage that the suspended sediment concentrations are markedly high.

3-1-2 Process of dune development

The observation on the bedform development through the Plexiglas wall and the change of flow patterns near the water surface indicated that the development of dunes has strong influence

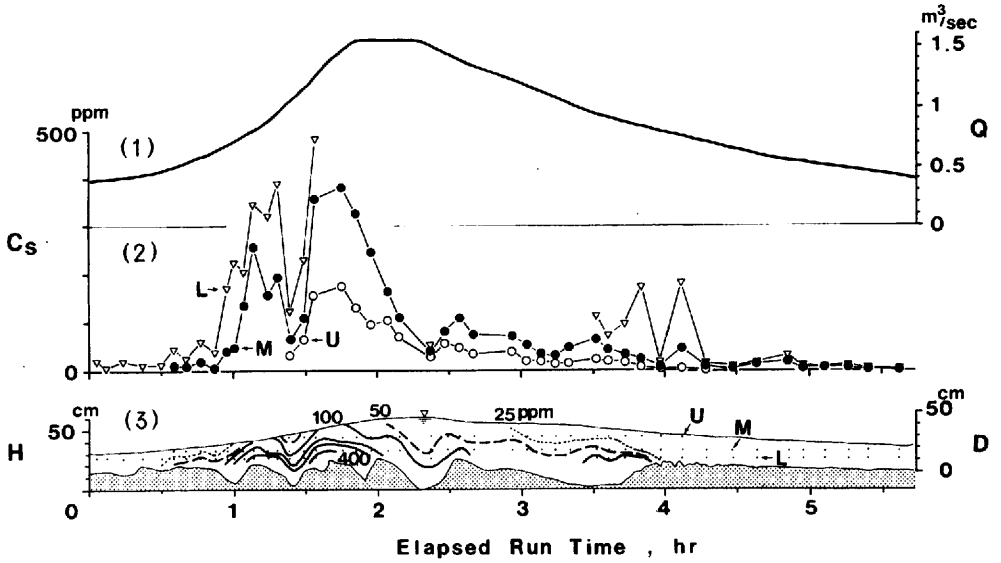

Fig. 7 Graphs showing temporal changes in water discharge, suspended sediment concentration and sand surface height in Case 1.

(1) Water discharge change with time.

(2) Variation of suspended sediment concentration at three different depths.

(3) Changes in distribution of suspended sediment concentration and in sand surface height at the sampling point of suspended sediment. Isopleth values show suspended sediment concentration in ppm.

C_S : suspended sediment concentration

D : mean water depth

H : height above the datum level

Q : water discharge

L, M, U: lowermost, middle and uppermost sediment sampling depth respectively

on sediment suspension.

Longitudinal profiles of the bed surface in a 6-m long subsection of the Plexiglas wall were drawn at frequent intervals throughout the run to trace the migration of each dune. The results are shown in Figs. 8-2, 8-3, 8-4 and 8-5. Data on the length and height of dunes obtained through the side window may be less accurate because of the wall effect and of the short length profile. However, the tendency of bedform changes during a runoff event can be clearly illustrated from these data without problem.

The process of dune development during a runoff event was characterized by four stages as denoted at the uppermost part of Fig. 8-2.

I Stage of low relief dune formation

Shortly after the initiation of the bed material movement, the bedform started to develop. The initial bedform at the minimum discharge was small dunes with low amplitide. Figure 8-2 shows that some dunes caught up their downstream adjacent dunes to make longer dunes, and that some dunes gradually disappeared.

II Stage of large dune growth

This stage corresponds to the time of rapid increase in discharge. As the discharge increased,

the dunes became larger. These dunes moved downstream at a rate of 8 to 15 cm/min. This migration speed was twice as large as that of the dunes in the former stage (Fig. 8-5). The dune profile in this stage became gradually triangular with a sharp brinkpoint and the dunes at a given time were of the rather uniform size, as seen in the Plexiglas wall section. It should be noted that violent boils occurred periodically everywhere in the flume throughout the stage.

III Stage of dune elongation

With decreasing discharge, the increase in dune length still continued, while the dune height became smaller or remained as it was at the peak discharge (Figs. 8-3 and 8-4). The dune crest was rounded and the dune profile became irregular. Dune migrating speed also slowed down (Fig. 8-5). Although the bed configuration constituted large dunes, only small boils could be seen on the water surface with carefull observations.

IV Stage of dune deformation

During the final stage of flow recession, the large dunes formed in the previous stage still remained. Small dunes appeared on the back of these large dunes, where the water depth was small and the flow velocity was high. They moved onto the crest of residual large dunes as slowly as the small dunes formed in the stage I (Fig. 8-5).

As observed through the Plexiglas wall, changes in dune size lag behind changes in flow conditions. During the rising stage, the dune size corresponding to a particular discharge does not have enough time to develop before discharge will increase further, so that the dune size is smaller than the one required for equilibrium with instantaneous discharge. On the other hand, when discharge decreases, the flow can not fully alter in the short time period the large dunes to smaller ones which are in equilibrium state. As a result, the dune size is greater than it should have been for a given discharge.

The curve showing the relationship between the dune size and discharge in the falling stage always plotted above the curve in the rising stage. The time lag between bedform and discharge was first demonstrated experimentally by Simons & Richardson (1962), and such lags in dune size have been widely known in natural rivers and their tidally influenced lower reaches (reviewed in Allen, 1983). In the Sakura River, Ibaraki Prefecture, Iseya (1982a) also showed that dunes with smaller wavelength occurred when the discharge increased and those with larger wavelength appeared when the discharge decreased.

3-1-3 Relationship between suspended sediment concentration and dune development

The observation described above revealed that both the dune growth and the high suspended sediment concentration occurred during the rising leg of a flood hydrograph. To investigate the relationship between suspended sediment concentration and dune development, continuous changes of sand surface elevation were accurately measured at the sediment sampling point by the electric sand level gauge.

As shown in Fig. 7-3, no significant changes of the sand surface height occurred for a while after water was introduced into the flume. However, the sudden lowering of sand surface occurred after 50 min of elapsed run time, and then the sand surface elevation fluctuated up and down with three or four peaks until about 140 min. This indicates that successive dunes passed through the sampling point with certain intervals.

It was during this period that the suspended sediment concentration was extremely high.

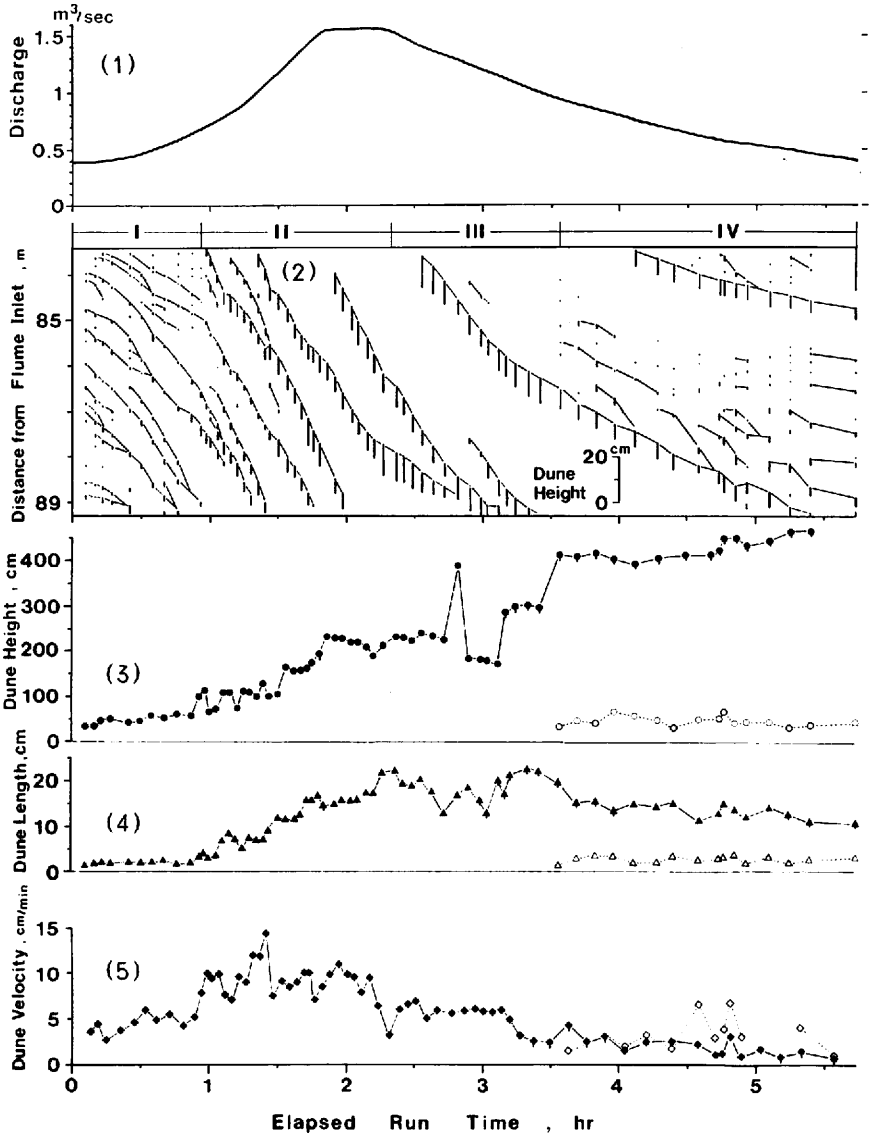

Fig. 8 Graphs showing the process of dune development in Case 1.

(1) Water discharge change with time.

(2) Diagram showing the migration of dune brinkpoint with time. Short vertical lines indicate the dune height, which was determined as the difference in height between dune brinkpoint and troughpoint.

(3) Dune length change in the window section (83.4 to 89.3 m from flume inlet). Open circules show average dune length of small dunes superposed on the large dune.

(4) Dune height change in the window section (83.4 to 89.3 m from flume inlet). Open triangles show average dune height of small dunes superposed on the large dune.

(5) Dune velocity change in the window section (83.4 to 89.3 m from flume inlet). Open squares show average dune velocity of small dunes superposed on the large dune.

Moreover, it should be noted that the suspended sediment concentration rapidly increased as soon as the first scour occurred on the sand surface.

As shown in Fig. 7-2, the change of suspended sediment concentration during this period has two peaks. This variation was caused by the presence of dunes. Figure 7-3 shows that the suspended sediment concentration is high over the crest part of dune, but is low over the trough part.

3.2 Runs with constant discharge (Case 2)

It was made clear from Case 1 experiment that the development of dunes must have a strong influence on sediment suspension. But the water surface slope as well as the water discharge were also changed in Case 1. Therefore, it was difficult to specify how much influence the dune development had on sediment suspension.

To make further investigations on this problem, six runs were performed in Case 2 with combination of different discharge (0.5, 1.0 and 1.5 m^3/sec) and bed slope (1/400 and 1/1,000) (Fig. 9). Not only water discharge but also water surface slope were kept constant during each run. Some of the results are tabulated in Tables 3 through 8. The generality of each run was confirmed by a supplementary experiment. In particular, Run 4 (discharge: 1.5 m^3/sec and slope: 1/400) was performed repeatedly, and detailed observations through the Plexiglas wall on the sedimentary structure and on the sediment transport manner were specially made during this run.

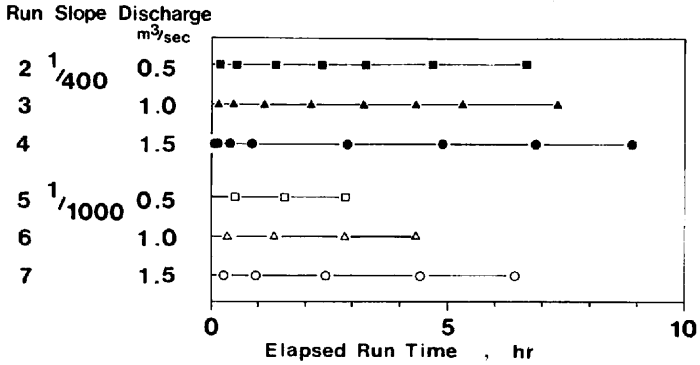

Fig. 9 Experimental conditions in Case 2. Experimental runs are indicated by different symbols, the location of which shows the time when bedforms were measured.

Table 2 Notation of symbols in Tables 3 through 8.

D	mean flow depth
Fr	Froude number
n	manning's roughness value (in metric unit)
Q	water discharge
S	water surface slope
T	elapsed run time
ΔT	run time of each step
T_e	time required to attain the equilibrium dune size
T_w	water temperature
U_*	shear velocity
V_D	dune velocity
V_m	mean flow velocity
V_s	surface flow velocity
λ	mean dune length
η	mean dune height
τ	shear stress
ω	stream power

Table 3 Experimental conditions and results (Run 2).

STEP	T min	ΔT min	Q 1/sec	S x 10^{-3}	T_w °C	D cm	V_s cm/sec	λ cm	η cm	λ/η	V_D cm/min
1	9	9	548	2.10	8.3	16.8	101	80.3	3.15	25.5	–
2	30	21	538	2.10	7.2	19.4	85.0	126	6.29	20.0	11.6
3	80	50	544	2.10	7.8	23.0	77.0	132	6.32	20.9	7.74
4	140	60	540	2.10	8.2	23.0	78.0	156	7.34	21.3	8.15
5	195	55	540	2.10	8.3	23.1	76.4	166	7.19	23.1	5.96
6	280	85	540	2.10	8.3	23.1	77.8	171	7.13	24.0	6.14

T_e = 150 min

STEP	V_m cm/sec	Fr	τ g/cm²	ω g/sec·cm	U_* cm/sec	n
1	81.5	0.635	0.0353	2.88	5.88	0.0171
2	69.3	0.503	0.0407	2.82	6.32	0.0222
3	59.1	0.394	0.0483	2.85	6.88	0.0291
4	58.7	0.391	0.0483	2.84	6.88	0.0293
5	58.4	0.388	0.0485	2.83	6.89	0.0295
6	58.4	0.388	0.0485	2.83	6.89	0.0295

Table 4 Experimental conditions and results (Run 3).

STEP	T min	ΔT min	Q l/sec	S $\times 10^{-3}$	T_W °C	D cm	V_S cm/sec	λ cm	η cm	λ/η	V_D cm/min
1	8	8	1010	2.45	9.2	22.4	135	93.1	5.15	18.1	–
2	27	19	997	2.45	9.2	29.7	105	139	8.85	15.7	14.7
3	67	40	990	2.45	9.2	33.1	96.7	171	10.1	17.0	9.51
4	127	60	994	2.58	9.5	34.1	91.5	224	11.9	18.8	9.16
5	194	67	981	2.32	9.7	34.9	94.3	238	13.1	18.2	8.38
6	258	64	996	2.45	9.6	34.9	90.9	258	12.7	20.4	8.18
7	318	60	993	2.45	9.6	34.5	98.3	253	13.6	18.6	6.08
8	438	120	996	2.45	9.9	34.5	–	251	13.6	18.5	7.58

T_e = 220 min

STEP	V_m cm/sec	Fr	τ g/cm²	ω g/sec·cm	U_* cm/sec	n
1	113	0.763	0.0549	6.20	7.33	0.0162
2	83.9	0.492	0.0728	6.10	8.44	0.0263
3	74.8	0.415	0.0811	6.07	8.91	0.0317
4	72.9	0.399	0.0880	6.41	9.29	0.0340
5	70.3	0.380	0.0810	5.69	8.91	0.0340
6	71.3	0.386	0.0855	6.10	9.15	0.0344
7	72.0	0.392	0.0845	6.09	9.10	0.0338
8	72.2	0.393	0.0845	6.10	9.10	0.0339

Table 5 Experimental conditions and results (Run 4).

STEP	T min	ΔT min	Q l/sec	S $\times 10^{-3}$	T_W °C	D cm	V_S cm/sec	λ cm	η cm	λ/η	V_D cm/min
1	3	3	1510	2.41	16.0	29.8	130	90.2	4.30	21.0	–
2	8	5	1490	2.41	15.8	34.5	127	121	7.21	16.8	–
3	23	15	1500	2.53	15.3	38.0	115	143	10.3	13.9	14.8
4	53	30	1500	2.24	15.3	40.9	108	172	11.3	15.2	11.4
5	173	120	1510	2.45	15.0	40.5	104	246	14.5	17.0	9.64
6	293	120	1480	2.48	15.0	39.6	108	337	18.6	18.1	9.69
7	413	120	1470	2.39	14.4	40.4	105	333	17.2	19.4	7.97
8	533	120	1470	2.37	14.5	39.5	104	342	18.0	19.1	8.40

T_e = 290 min

STEP	V_m cm/sec	Fr	τ g/cm²	ω g/sec·cm	U_* cm/sec	n
1	127	0.743	0.0718	9.12	8.39	0.0172
2	108	0.587	0.0831	8.98	9.03	0.0224
3	98.4	0.510	0.0961	9.46	9.71	0.0268
4	91.9	0.459	0.0916	8.42	9.48	0.0284
5	93.2	0.468	0.0972	9.06	9.86	0.0279
6	93.6	0.475	0.0982	9.19	9.81	0.0287
7	90.8	0.456	0.0966	8.77	9.73	0.0294
8	93.3	0.474	0.0936	8.73	9.58	0.0281

Table 6 Experimental conditions and results (Run 5).

STEP	T min	$\triangle T$ min	Q 1/sec	S $\times 10^{-3}$	T_W ℃	D cm	V_S cm/sec	λ cm	η cm	λ/η	V_D cm/min
1	30	30	540	0.830	15.0	22.1	71.3	76.7	2.12	36.2	–
2	90	60	540	0.855	15.0	23.4	69.4	80.1	2.23	35.9	–
3	170	90	540	0.781	15.2	24.2	65.1	78.9	2.32	34.0	–

T_e = 30 min

STEP	V_m cm/sec	Fr	τ g/cm²	ω g/sec·cm	U_* cm/sec	n
1	61.1	0.415	0.0183	1.12	4.24	0.0172
2	57.7	0.381	0.0200	1.15	4.43	0.0192
3	55.8	0.362	0.0189	1.05	4.30	0.0194

Table 7 Experimental conditions and results (Run 6).

STEP	T min	$\triangle T$ min	Q 1/sec	S $\times 10^{-3}$	T_W ℃	D cm	V_S cm/sec	λ cm	η cm	λ/η	V_D cm/min
1	20	20	1070	0.995	14.2	34.6	87.3	75.4	3.17	23.8	–
2	80	60	1040	1.23	14.2	37.5	82.2	99.7	3.93	25.4	3.08
3	170	90	1040	1.15	14.3	37.9	80.0	94.8	4.31	22.0	2.83
4	260	90	1040	1.01	14.3	38.8	78.7	99.7	4.26	23.4	2.64

T_e = 80 min

STEP	V_m cm/sec	Fr	τ g/cm²	ω g/sec·cm	U_* cm/sec	n
1	77.3	0.420	0.0344	2.66	5.81	0.0201
2	69.3	0.361	0.0461	3.20	6.72	0.0263
3	68.6	0.356	0.0436	2.99	6.54	0.0259
4	67.0	0.344	0.0392	2.63	6.20	0.0252

Table 8 Experimental conditions and results (Run 7).

STEP	T min	$\triangle T$ min	Q l/sec	S $\times 10^{-3}$	T_W °C	D cm	V_S cm/sec	λ cm	η cm	λ/η	V_D cm/min
1	16	16	1410	0.953	13.0	34.4	82.3	80.7	4.26	18.9	–
2	56	40	1410	0.953	13.0	44.1	87.3	111	5.62	19.8	–
3	146	90	1480	0.953	13.2	47.4	87.2	147	8.13	18.1	5.16
4	266	120	1480	1.05	14.0	48.3	84.1	167	9.66	17.3	3.72
5	386	120	1490	1.07	13.8	47.7	84.6	172	10.3	16.7	4.25
6	506	120	1490	1.07	14.3	48.0	–	179	10.4	17.2	–

T_e = 275 min

STEP	V_m cm/sec	Fr	τ g/cm²	ω g/sec·cm	U_* cm/sec	n
1	102	0.555	0.0328	3.34	5.67	0.0149
2	79.9	0.384	0.0420	3.66	6.42	0.0244
3	78.1	0.361	0.0455	3.55	6.67	0.0241
4	76.6	0.352	0.0507	3.88	7.05	0.0260
5	78.1	0.361	0.0510	3.99	7.07	0.0256
6	77.6	0.358	0.0480	3.72	7.09	0.0258

3-2-1 Process of dune development

a. Changes in dune length and height

It was found that changes in bed configuration can be classified into two stages. One is "Developing dune stage" and the other is "Equilibrium dune stage". Figure 10 shows successive changes of mean dune length and height for six different runs. Both length and height of dunes increase gradually in the developing dune stage. Meanwhile, they are almost constant in the equilibrium dune stage. Dune length/height ratios of each run, however, have little change throughout the run (Fig. 10). This indicates that a similar profile of dune is maintained in the developing dune stage as well as in the equilibrium dune stage.

It should be noted that each run has a peculiar time to attain the equilibrium dune size. The time required to attain the equilibrium dune size, T_e, in Fig. 10 will be discussed later. The quantity T_e was determined as indicated in Fig. 11.

b. Changes in the bedform and the flow condition

Taking Run 4 as an example, changes in the bedform and the flow condition are described in detail. Measurements of bedforms were made 8 times (Steps 1 to 8) in this run. Steps 1 to 6 are in the developing dune stage and Steps 7 and 8 are in the equilibrium dune stage. The plan view of bedforms at the end of each step is shown in Fig. 12. Each step is characterized as follows:

Step 1 When the flow was established on the carefully planed sand surface, the water depth was shallow and the flow velocity was large as the resistance to flow was very low and the water surface slope was rather high. In a little while, standing waves occurred on the water surface and the waving bedforms with very low amplitude started to develop. Their spacing was nearly equal to the wavelength of standing waves. The water surface was in phase with the bed surface except when an standing wave broke. This early bedform resembled "antidune" described by Kennedy

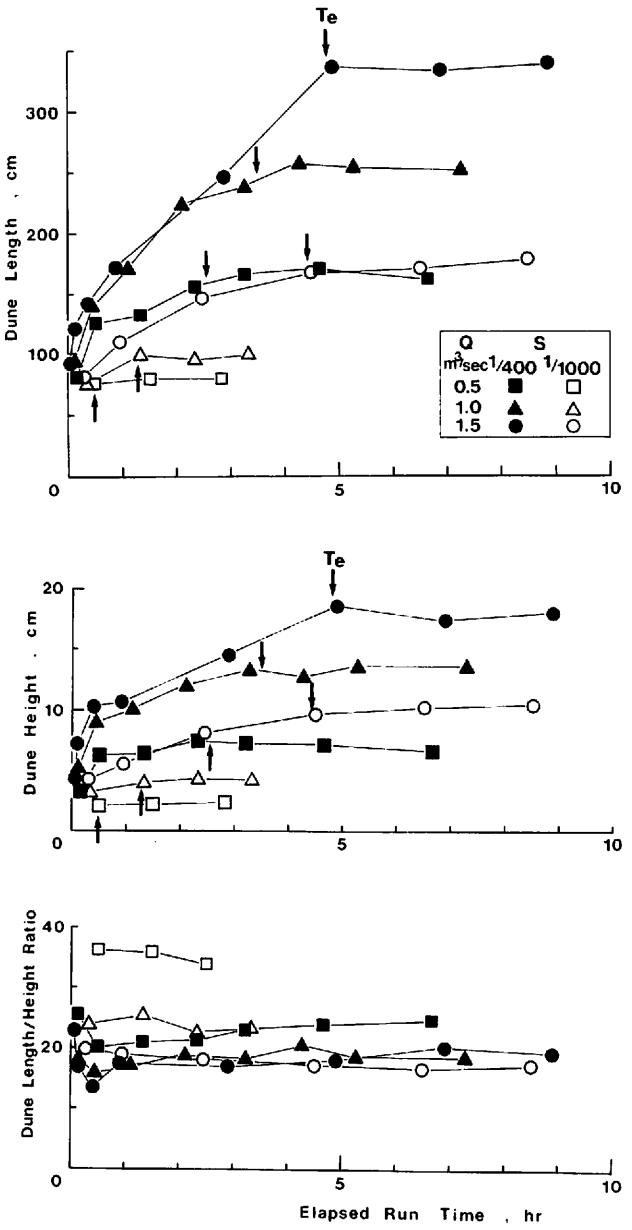

Fig. 10 Successive changes of dune size in Case 2. Arrows show the time when dunes attain equilibrium sizes. For symbols, see Fig. 9.
T_e: time required to attain the equilibrium dune size

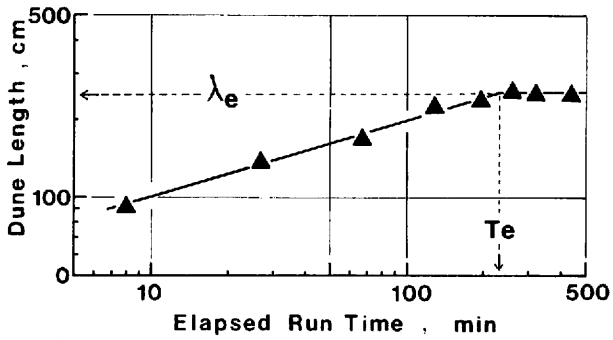

Fig. 11 Graph showing how to determine the values of T_e and λ_e (Run 3, Q = 1.0 m³/sec, S = 1/400). Dune length vs. time curve of each run, plotted in a log-log paper, has a sharp break. The abscissa value corresponding to this point is defined as T_e. T_e: time required to attain the equilibrium dune size, λ_e: equilibrium dune length

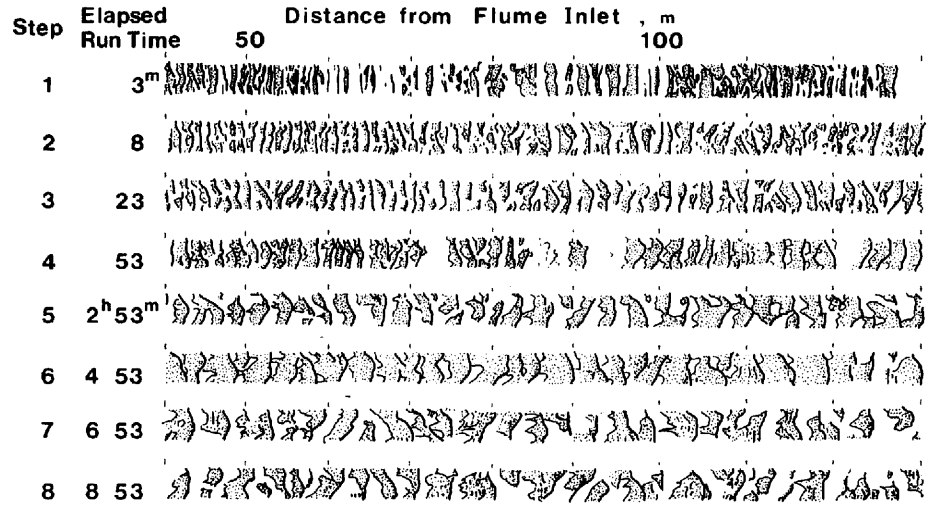

Fig. 12 Plan view of bedforms at the end of each step in Run 4. Blank areas indicate submerged part after incomplete drainage.

(1963). Standing waves on the water surface were soon disappeared.

Step 2 The flow depth increased and the flow velocity decreased as the bed resistance increased with the bedform development. In this period, the sand wave had an usual triangular shape and could be called "dune". Two-dimensional dunes were formed with their crest lines being mostly perpendicular to the flow direction. Some of dunes caught up their downstream next dunes to make longer dunes.

Step 3 The bed condition of this step was similar to that of Step 2. Boils associated with the

dunes began to appear on the water surface, but they were not so violent as in Step 4.

Step 4 Scouring of the dune troughs gradually became intense and dune shapes gradually became three-dimensional. Violent boils began to appear on the water surface.

Step 5 Very strong eddies lifted sand particles from the bed to the water surface. These eddies resulted in large boils at the water surface. Dune crest lines were sinuous across the flume. Dune troughs were scoured intensely and the amplitude of dune increased. Dune trough had a basin-like concave upward shape and scour holes were conspicuous in various places after draining from the flume (Fig. 13).

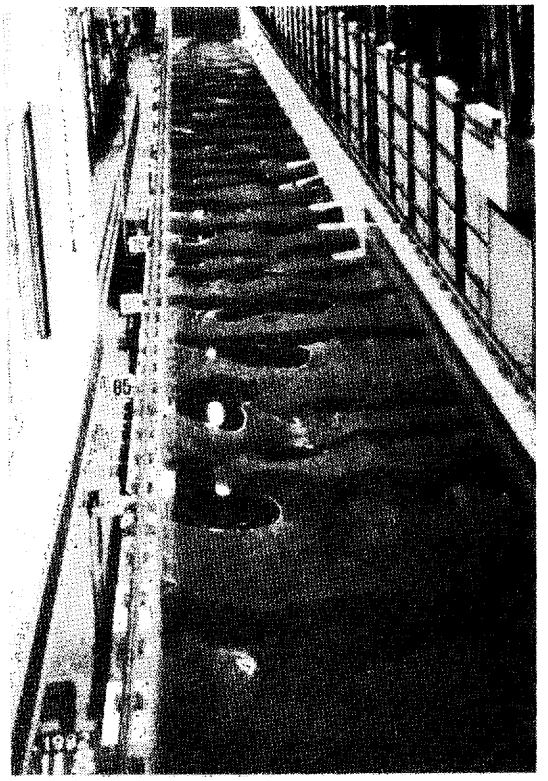

Fig. 13 Upstream view of dunes at the end of Step 5 of Run 4.

Step 6 The dunes in this step were somewhat larger in amplitude and more widely spaced than those in Step 5. Turbulence at the water surface seemed to be less than in Step 5, although many boils were still observed.

Step 7 The length and height of dunes were not so different from those in Step 6. There was a sharp topographic break of slope between the slipface and the bottomset of dunes. Small dunes could be seen on the back of large dunes. The water surface showed weak boil activities.

Step 8 Bedform and flow condition in this step were similar to those in Step 7.

Such changes in bed condition as described above can be also seen in Figs. 14-2 and 15-2,

which show the temporal variations both of the water surface level and of the sand surface elevation at the sampling point of suspended sediment. The sand surface elevation at a fixed point fluctuated up and down as dunes migrated downstream. The sand surface level had fairly regular oscillation with low amplitude for about an hour after the start of run (Steps 1 to 4 in Fig. 14-2). This suggests that two-dimensional dunes with low relief successively passed through the sampling point (see Fig. 12). On the other hand, the temporal variations of sand surface height in Steps 5 and 6 have rather irregular pattern with large amplitude. This indicates that much larger dunes developed on the bed surface.

The water surface height gradually increased until about an hour of elapsed run time. After this time, however, the water surface stayed at nearly the same height, although the bed roughness increased as large dunes developed on the bed surface. Water surface undulation was always out of phase with the bed configuration.

The patterns of dune development in other five runs resembled more or less those in Run 4 (Figs. 25 to 29 in Appendix A). In general, the changes in bed configuration and flow characteristics at a constant discharge can be summarized as follows:

For only a few minutes after the start of a run, the water depth is small and the flow velocity is high because of only grain roughness, and standing waves occur on the water surface. In the developing dune stage, small dunes of low amplitude are formed with crest lines being nearly straight across the flume; these dunes grow larger dunes with undulated crest lines. Scour on the dune trough causes the increase of dune amplitude. It should be noted that violent boils associated with the dune development occur periodically on the water surface.

On the other hand, in the equilibrium dune stage, the dimensions of dunes become stable. It should be noted that boils on the water surface are relatively indistinct in spite of the existence of very large dunes on the sand surface.

3-2-2 Variation of suspended sediment concentration

Suspended sediment concentrations for six runs were continually measured and the measurement confirmed that the development of dunes has a strong influence on the change of suspended sediment concentration, even if the discharge and the slope are kept constant. Namely, it is found that suspended sediment concentration is higher during the developing dune stage than during the equilibrium dune stage.

Taking Run 4 as an example, the variation of suspended sediment concentration in each stage is described. Figures 14-1 and 15-1 show the successive changes of suspended sediment concentration at three different depths in Run 4. The results of other five runs are shown in Appendix A and Appendix B.

a. Variation of suspended sediment concentrations in the developing dune stage

In the developing dune stage, the flow contained relatively large amount of suspended sediment, and suspended sediment concentrations measured at all three different depths greatly varied with time (Fig. 14-1). In particular, a drastic change occurred during Step 5, in which the maximum concentration of suspended sediment was five times as large as the minimum even at the uppermost sampling depth. These marked temporal variations of suspended sediment concentration were caused by the spatial distribution of suspended sediment over the dune bedforms. In fact, suspended sediment concentration was especially high when the violent boils could be

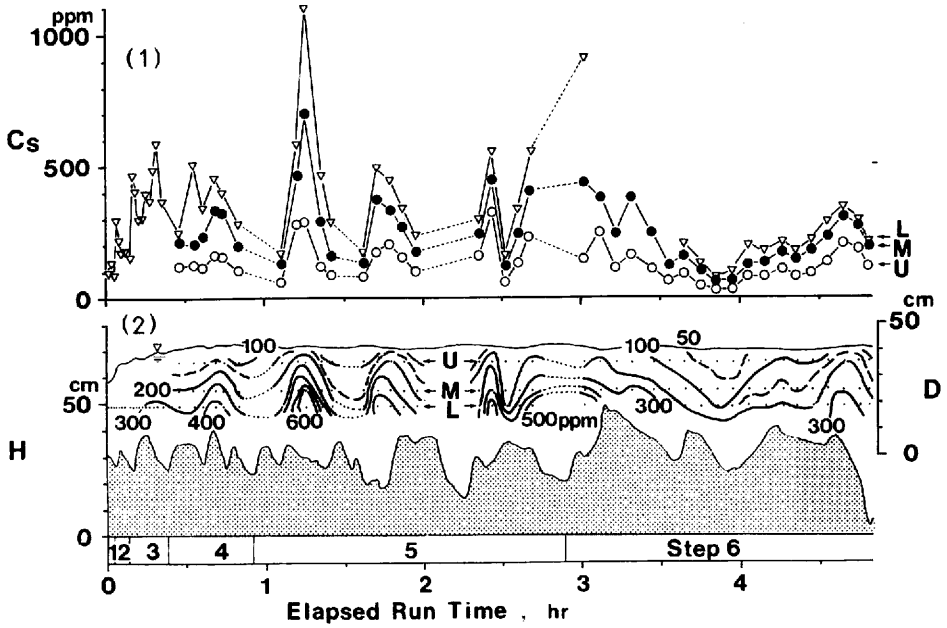

Fig. 14 Temporal variation of suspended sediment concentration in the developing dune stage for Run 4.

(1) Successive changes of suspended sediment concentration at three different depths.

(2) Isopleths of suspended sediment concentration.

C_S : suspended sediment concentration

D : mean water depth

H : height above the datum level

L, M, U : lowermost, middle and uppermost sediment sampling depth respectively

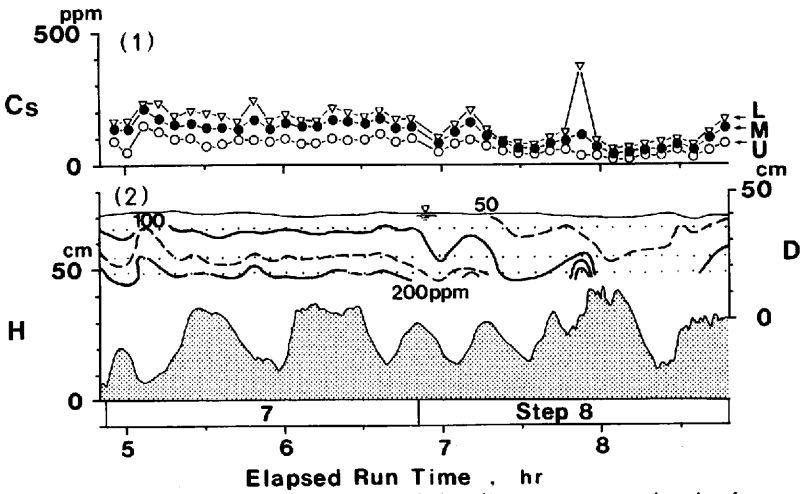

Fig. 15 Temporal variation of suspended sediment concentration in the equilibrium dune stage for Run 4. For symbols, see Fig. 14.

(1) Successive changes of suspended sediment concentration at three different depths.

(2) Isopleths of suspended sediment concentration.

seen around the sampling equipment, where the suspended sediment particles carried by strong eddies were sampled through the siphon nozzle.

However, from Fig. 14 only, it is difficult to make clear the correlation between dune shapes and the spatial distribution of suspended sediment concentration. Because the phenomenon has three-dimensional nature. Visual observation on the sediment movement over dunes through Plexiglas wall qualitatively indicated that the suspended sediment concentration was higher over the crest portion of dunes than over the trough portion. No sooner the intense scour occurred near the reattachment point of a dune by attacking the strong current separated from the crest of an upstream dune than the strong eddies were generated and moved upward into the main part of the flow with picking up a large amount of sediment particles on the bed surface.

b. Variation of suspended sediment concentration in the equilibrium dune stage

The flow in the equilibrium dune stage contained relatively small amount of suspended sediment, while the discharge and the water surface slope remained constant (Fig. 15 and Table 5). Moreover, suspended sediment concentration had little variation with time, although many dunes with large amplitude successively passed through the sampling point.

It was already described that only weak boils could be seen on the water surface in Steps 7 and 8. This means that generation of eddies on the stoss side of dunes declines in the equilibrium dune stage. Accordingly, sporadic high concentration of sediment brought up by eddies can be seen no more.

c. Vertical distribution of suspended sediment

As shown in Fig. 16, the vertical distribution of suspended sediment concentration seems to follow the conventional distribution law (Rouse, 1937; Einstein, 1950). The average suspended sediment concentration of each sampling depth in the developing dune stage is twice as large as that in the equilibrium dune stage.

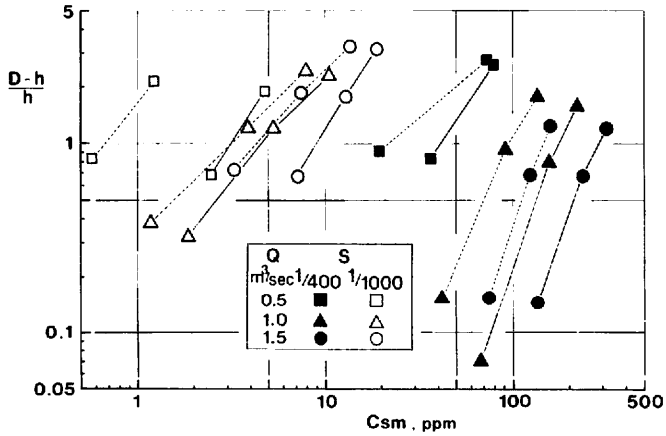

Fig. 16 Suspended sediment concentration plotted against relative height above the stream bed in Case 2. Solid lines indicate the developing dune stage and dotted lines indicate the equilibrium dune stage. For symbols, see Fig. 9.
C_{sm} : mean concentration of suspended sediment
D : mean water depth
h : sampling height above the mean bed

3-2-3 Changes in flow characteristics

Visual observations on flow characteristics through the Plexiglas wall and from the air qualitatively indicated that strong eddies which contained a large amount of suspended sediment periodically occurred in the developing dune stage, and such eddies became rather indistinct in the equilibrium dune stage. Measurements of instantaneous velocity fluctuations using the sonic current meter were made in such a flow field.

Figures 17 and 18 show the turbulent flow statistics of Run 4. The velocity U is the compound flow component in the x-y plane, and Θ is the angle between the direction of U and the x-axis which is in the longitudinal direction of the flume. The velocity W is the vertical component of turbulent flow. Thus, the instantaneous velocity components and angle (U, W, Θ) can be expressed as the sum of mean value ($\overline{U}$, $\overline{W}$, $\overline{\Theta}$) and the instataneous fluctuations from the mean (u', w', θ'):

$$U = \overline{U} + u'$$

$$W = \overline{W} + w'$$

$$\Theta = \overline{\Theta} + \theta'$$

Generally speaking, the increase or decrease of time-mean-flow velocities, $\overline{W}$ as well as $\overline{U}$, had a close relation to dune shape, whenever dunes were in the developing stage or in the equilibrium stage. The mean velocity $\overline{U}$ increased over the dune crest and decreased over the dune trough; $\overline{W}$ decreased over the leeside slope of dune and took a minimum value over the dune trough point, and reverse relation existed along the stoss side slope of dune. Such changes in $\overline{U}$ and $\overline{W}$ are caused by the contraction and expansion of the flow over the dunes as it has been usually stated (Raudkivi, 1967, p. 199-208). Namely, the flow is thought to accelerate along the upstream slope of dunes and decelerate over the trough portion.

The magnitude of turbulent fluctuations, however, is quite different between the two dune stages (Figs. 17 and 18). The magnitude of turbulent fluctuation is given by the standard deviation of the velocity component (σ_i, i = U, W, Θ). In the developing dune stage, the values of standard deviations of U and W changed widely and they were the largest when $\overline{U}$ was the minimum peak and $\overline{W}$ was the maximum peak. Moreover, at this particular time, the flow direction, Θ, also changed with moderate departures from the mean value, although it was usually in the main axis of the flume. These results suggest the existence of intensely fluctuating and rotating flows, that is, of the eddy motion. In the equilibrium dune stage, on the contrary, U and W usually changed with nearly fixed small departures from their means.

The immersed weights of suspended particles are supported by the vertical flow component of turbulent flow. As shown in Figs. 19 and 20, it is the changes of σ_W, an index of upward fluctuation of turbulent flow, and not the change of time-mean velocity, $\overline{W}$, that agrees well with the spatial distribution of suspended sediment concentration.

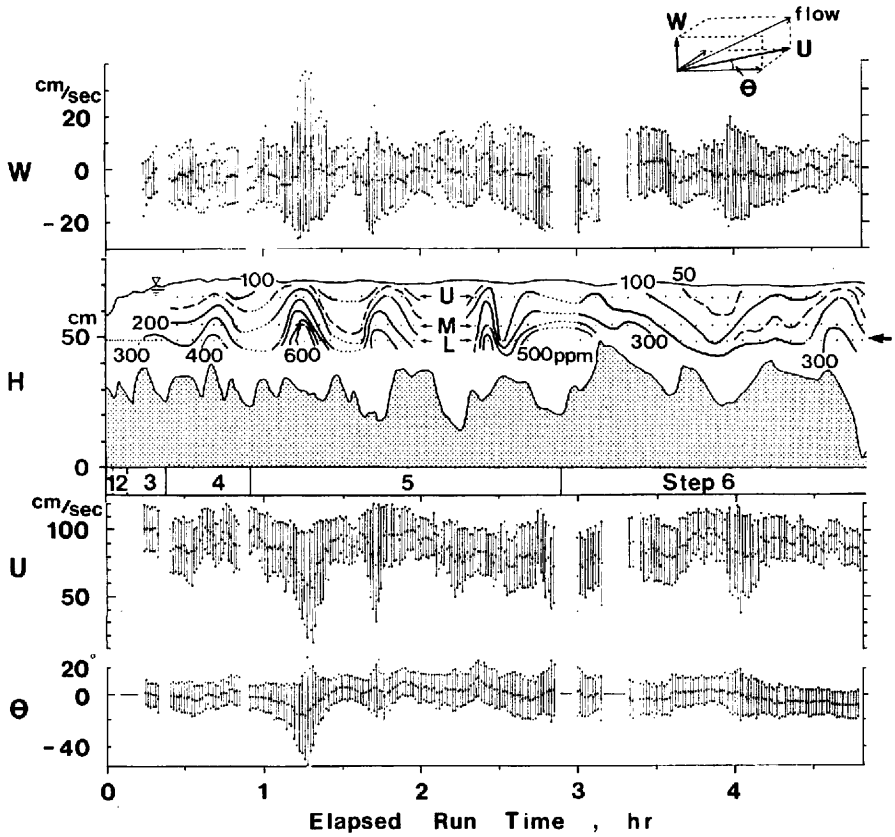

Fig. 17 Characteristics of turbulent flow change in the developing dune stage for Run 4. Vertical lines show the magnitude of turbulent fluctuations. Each line extends from $-2\sigma_i$ to $+2\sigma_i$ ($i = U, W, \Theta$) in relation to the average value. A center circule of each line is one-minute average value of the instantaneous flow characteristics ($\overline{U}$, $\overline{W}$, $\overline{\Theta}$).The arrow indicates the elevation of a sensor of sonic current meter.

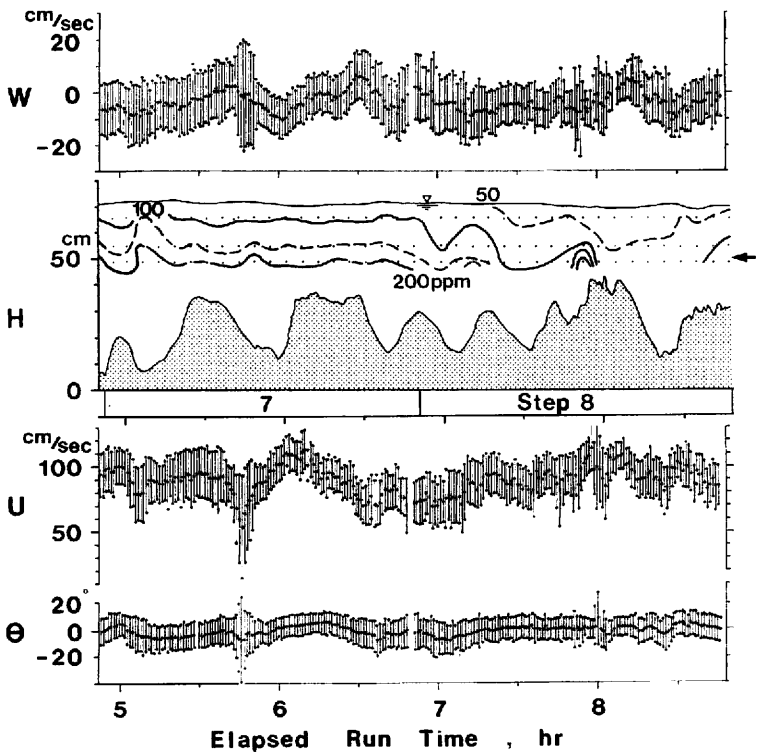

Fig. 18 Characteristics of turbulent flow change in the equilibrium dune stage for Run 4. Explanation is given in Fig. 17.

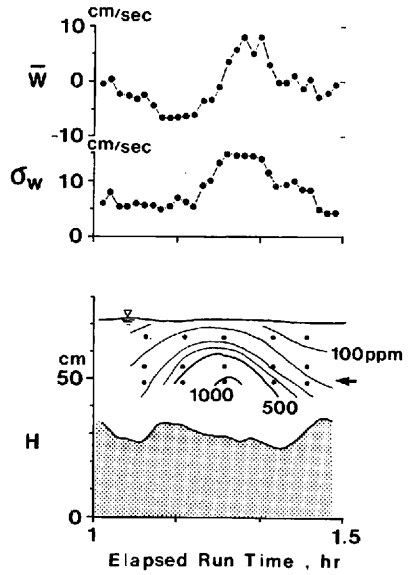

Fig. 19 Changes in vertical flow component and distribution of suspended sediment concentration in the developing dune stage for Run 4. The arrow indicates the elevation of a sensor of sonic current meter.

$\bar{W}$: time-average value of vertical flowcomponent

σ_W : standard deviation of vertical flowcomponent

H : height above the datum level

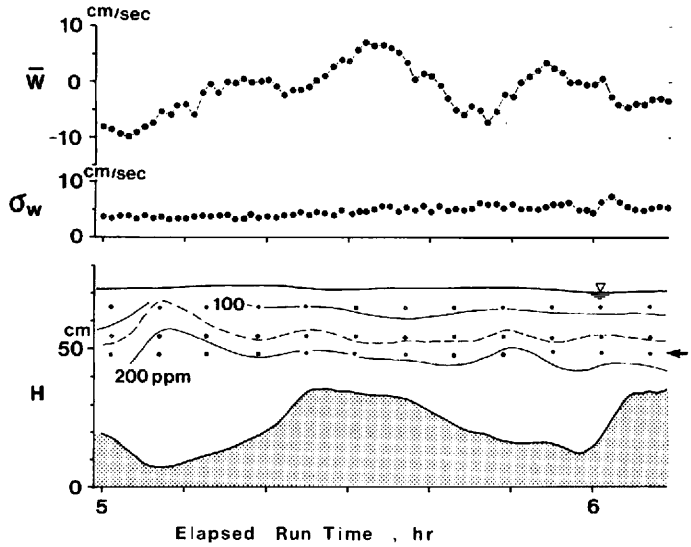

Fig. 20 Changes in vertical flow component and distribution of suspended sediment concentration in the equilibrium dune stage for Run 4. Explanation is on Fig. 19.

CHAPTER IV

DISCUSSION

4-1 Cause of the high suspended sediment concentration in the developing dune stage

In the developing dune stage, strong eddies associated with the dune growth lift a large amount of sediment particles from the bed surface to the main flow. This causes the high suspended sediment concentration in this stage.

Since the study of Matthes (1947), the upward transport of a large amount of sediment by eddies or by kolks has already been described in some natural rivers (Korchokha, 1968; Coleman, 1969; Jackson, 1976). Guy et al. (1966) also pointed out such mechanism of sediment suspension in their intensive experimental works. From these studies added to existing experimental investigations of fluid motions in turbulent boundary layers (for example, Kline et al., 1967; Nychas et al. 1973; Offen & Kline, 1975), Jackson (1976) emphasized that the bursting process in turbulent boundary layers may play an important role in the sediment suspension.

In the present experimental study, it was found that the bursting process accompanied by strong eddies was dominant in the developing dune stage, but that such a process declined in the equilibrium dune stage. Further studies on the relationship between the turbulent flow structure and the bedform development under unsteady flows are necessary to elucidate the cause of this phenomenon.

4-2 Time required to attain the equilibrium dune size

The flows in natural rivers change in their direction and magnitude with space and with time. These changes occur rapidly during a runoff event. A delayed response of the bedform to the flow characteristics change, has been observed in many rivers and examined experimentally. Promising methods to predict the change in dune dimensions by means of mathematical modeling have been proposed by Allen (1976a, b, c, 1978) and Fredsøe (1979, 1981). However, it is not yet possible to estimate how long it takes for the bedform to respond the flow change.

4-2-1 Equilibrium dune length and height

It is commonly said that the wavelength of dunes is determined by the flow depth. Yalin (1973, p. 222-232) estimated that a ratio of dune wavelength to flow depth in the steady uniform flow is equal to 2π. This estimation is based on the concept that the periodicity of macroturbulence, when it is expressed as a wavelength, matches with the dune wavelength. Jackson (1976) indicated that dune lengths fell between 4 to 9 times the corresponding flow depths. He analized the data obtained not only from flume experiments but also rivers and marine environments. An average ratio of dune length to depth, about 7 or 8, from his figure agrees well with Yalin's ratio.

However, the data of Case 2 in the present experiment widely scatter when dune lengths in the equilibrium stage are plotted against the water depths (Fig. 21). The dune lengths on a steep slope are always larger than those on a gentle slope.

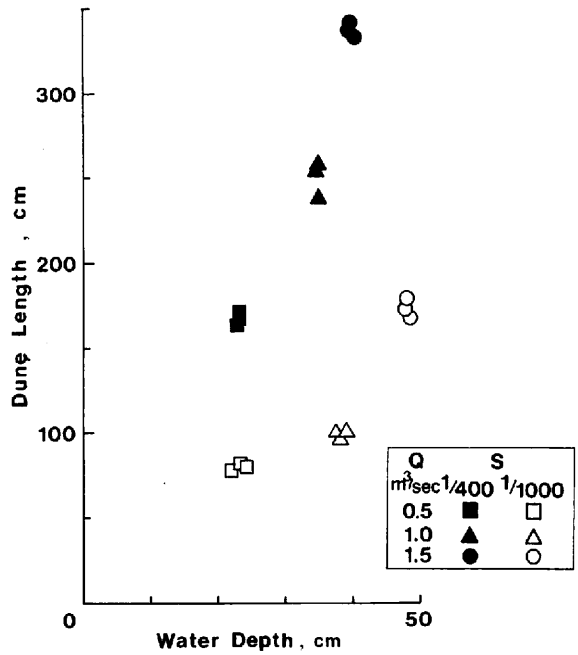

Fig. 21 Dune length vs. mean flow depth in the equilibrium dune stage of Case 2. For symbols, see Fig. 9.

It is empirically found that the equilibrium dune length has a good correlation with the stream power, ω (Fig. 22). The stream power is described as

$$\omega = \tau_0 V_m = \gamma_f q S$$

where τ_0 is the boundary shear stress ($= \gamma_f DS$), V_m is the mean flow velocity, D is the flow depth, S is the gravity gradient or the water surface slope, q is the water discharge per unit width, and γ_f is the specific weight of water (Bagnold, 1966). In this experiment, the stream power is an independent variable because both discharge and slope are controlled.

The stream power is a rate of energy input per unit bed area. It must be partly dissipated in transporting the bed material accompanied by the formation of dunes, while it is mostly dissipated in maintaining the flow. Therefore, the close relation between the dune length and the stream power in Fig. 22 might be an acceptable explanation.

The dune height also shows a good relation with the stream power (Fig. 23). Because the dune height grows in harmony with dune length as described in the section of 3-2-1-a.

4-2-2 Relationship between the time required to attain the equilibrium dune size and the stream power

We shall consider that equilibrium dunes having length λ_e, and height η_e, are formed on the initial flat bed condition. To simplify the analysis, it is assumed that the integral sediment dis-

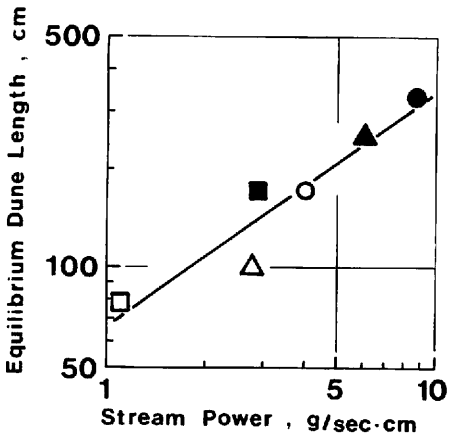

Fig. 22 Correlation between equilibrium dune length and stream power in Case 2. For symbols, see Fig. 9.

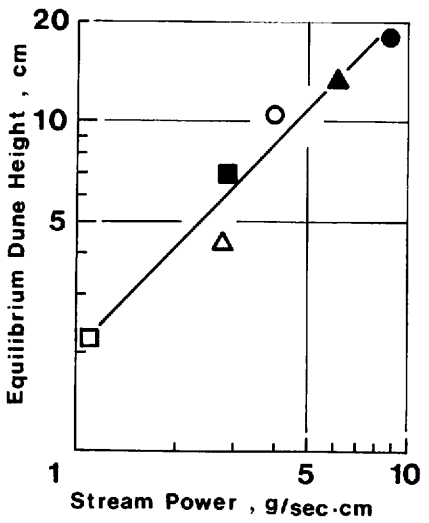

Fig. 23 Correlation between equilibrium dune height and stream power in Case 2. For symbols, see Fig. 9.

charge per unit width, q_S, necessary for the attainment of equilibrium dune is proportional to the area of equilibrium dune profile:

$$q_S \sim \alpha_1 (1-\epsilon) (\gamma_S - \gamma_f) \lambda_e \eta_e$$

where ϵ is the porosity, γ_S and γ_f are the specific weights of solid and fluid respectively, and α_1 is a coefficient.

The water discharge, q, and the water surface slope, S, give the flow energy at work in the flume. The flow energy per unit time and unit width is after all the stream power ($= \gamma_f qS$). Therefore, the total energy input before the formation of equilibrium dunes can be expressed as

$$\omega \cdot T_e$$

where T_e is the time required to attain the equilibrium dune size.

As a part of this energy supply must be dissipated for transporting the bed material to form dunes, the following equation is obtained:

$$\alpha_1 (1-\epsilon) (\gamma_S - \gamma_f) \lambda_e \eta_e \sim \alpha_2 \omega T_e .$$

Thus,

$$T_e \sim \frac{\alpha_3}{\omega} \lambda_e \eta_e$$

where α_2 and α_3 are coefficients.

The equilibrium dune length and height are respectively given in Figs. 22 and 23 as

$$\lambda_e \sim \omega$$

and

$$\eta_e \sim \omega .$$

Therefore, the following relation is finally obtained:

$$T_e \sim \omega .$$

The correlation of T_e and ω was tested using the data of six runs in Case 2 and the result was given in Fig. 24. Figure 24 means that the larger the stream power is, the longer time it takes to attain the equilibrium dune size.

In the case of varying flow conditions like Case 1, the stream power increases as the water discharge increases. Therefore, it is reasonable to state that the rising stage of Case 1 is always in the developing dune stage.

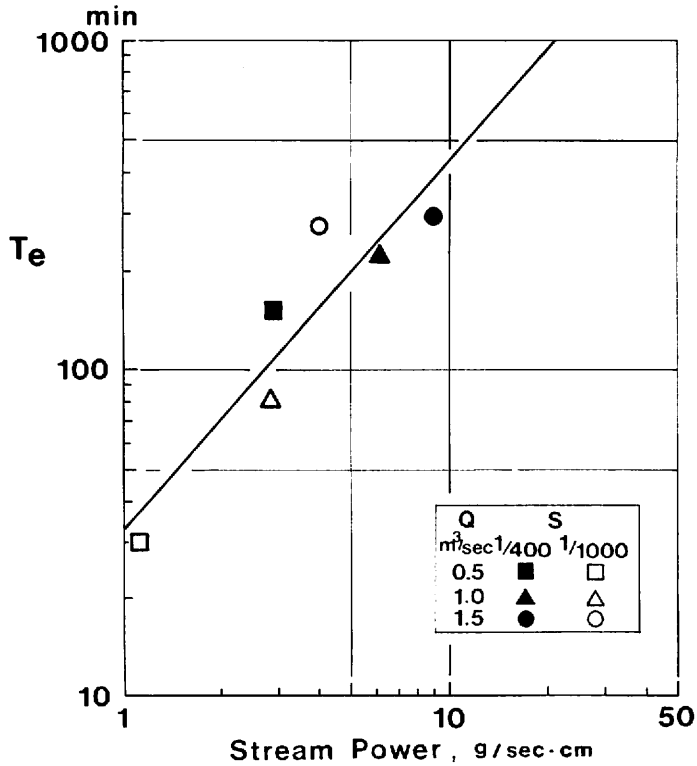

Fig. 24 Relationship between stream power and time required to attain the equilibrium dune size, T_e, in Case 2. For symbols, see Fig. 9.

4-3 Bed conditions in natural sand-bed rivers

Sediment movement causes the formation of bedforms. Bedforms which develop under all flow conditions in the laboratory flume can be predicted from bedform phase diagrams such as the stream power-grain size graph by Simons et al. (1965), the bed shear stress-grain size graph by Leeder (1982), the nondimensional shear stress-grain size graph by Allen (1983) and the flow velocity-flow depth-grain size graphs by Southard (1971) and by Costello & Southard (1981). However, these diagrams can not be always applied to the bedform of natural rivers. One of the most important reasons would probably be that bedform phase diagrams define the existence of bedforms under steady state equilibrium conditions. Meanwhile, unsteady and/or nonuniform flow conditions are usual in the field. Bedform history is also important in the natural rivers.

The flume experiments in this paper were conducted only such hydraulic conditions that dunes in the lower flow regime developed on the smoothed bed. This experimental condition can be sufficiently applicable to the field condition. Because many field observations have been revealed that dunes are the most prevailing bedform in the sand-bed river channels. In Japan, bedform measurements using the echo sounder were made in such rivers as the Edo (Tsuchiya, 1971), the Hii (Tsuchiya, 1971), the Yoro (Mezaki, 1973) and the Ishikari (Takagi et al., 1982). The data show that dunes are formed on the bed surface during the floods. Conversely, during the low-water level period, it is usually seen that the sand surface is fairly even, although ripples or small dunes occupy in the deeper thread of a stream. Based on echo-sounding surveys in the Teshio River, Hokkaido, Ikeda and Iseya (1980) also showed that large dunes occurred on the bed surface during a flood, and that the sand surface was moderately smooth during a low flow season in spite of 4- to 5-m flow depth.

4-4 Application of experimental results to natural sand-bed rivers

A small water depth in the laboratory flume requires a steep slope to get a large stream power. While, a large water depth gives the same stream power in a natural river which has a gentle slope. Therefore, the relation in Fig. 24 will not be able to extraporate to the natural flow of greater depth and gentler slope, without considerable modification. However, the general relation that the larger the stream power is, the longer time it takes to attain the equilibrium dune size will be expected to apply to the natural environment.

In a natural river channel, the stream power at a station increases mainly due to an increase in the water discharge. Therefore, roughly speaking, the dune developing stage would be always present in the rising leg of a flood hydrograph in which the water discharge increase rapidly enough. The active growth of dune dimensions in the rising leg of a runoff event has a notable effect on sediment suspension, and causes the high suspended sediment concentration.

Flow characteristics on the water surface were observed during large floods in several sand-bed rivers, such as the Tone, the Edo and the Kinu Rivers. In these rivers, it took only one or two days to reach the peak discharge and the water discharge usually changed over a few 100-folds range. Many periodical violent boils were frequently observed across the width of a channel during the rising stage. The area of surface boils was dark black as compared with the adjacent quiescent area. This turbidity contrast indicates that surface boils are abundant in sand particles lifted by strong eddies, which are commonly observed as upwelling of more turbid water. On the other hand, during the falling stage, the water surface was relatively placid and only weak boils could be seen. These changes of the surface flow pattern depending on rising and falling flood stages are

very similar to those observed in the flume.

These observations on the surface flow characteristics in the rivers strongly suggest that dune dimensions increase in response to a rapid increase of water discharge, and that such dune development affects the macro turbulent flow structure to suspend a large amount of sediment particles.

CHAPTER V

SUMMARY AND CONCLUSION

In order to examine a possible relation between the sediment suspension and the bedform development, the flume experiments were carried out under such hydraulic conditions that dunes in the lower flow regime developed on the initially flat bed.

Results are summarized as follows:

(1) The flume test simulating a runoff event confirmed the fact that the concentration of supended bed material load (referred to as the "suspended sediment" in this paper) are greater on the rising leg than on the falling leg of a runoff event in the natural sand-bed rivers.

(2) It was found that the development of dunes has a strong influence on sediment suspension. Namely, the suspended sediment concentration rapidly increases as soon as the first scour occurs on the back of dune and the concentration becomes extremely high as larger dunes are developed by the increasing discharge. During this period, violent boils appear periodically everywhere on the water surface.

(3) With decreasing flow discharge, scours on the stoss side of dunes do not occur any more and the dune troughs are gradually buried. Conspicuous boils can not be observed.

(4) Other six different runs, in which the water discharge was held constant, were performed to make further investigations on the effect of dune development to the sediment suspension. These experiments indicate that changes in the bed configuration can be classified into two stages. One is "Developing dune stage" and the other is "Equilibrium dune stage".

In the developing dune stage, small dunes of low amplitude which have relatively straight crest lines across the flume, grow into larger dunes with sinuous crests. It should be emphasized that scours on the back of dunes cause the increase of dune amplitude and that violent boils associated with the dune growth occur periodically on the water surface.

In the equilibrium dune stage, not only dune length but also dune height do not change so much. Boils on the water surface are rather indistinct although very large dunes exist.

(5) Continual measurement of suspended sediment concentration shows that the suspended sediment concentration are higher in the developing dune stage than in the equilibrium dune stage. In the former dune stage, the fluid mass containing large amounts of sediment particles are advected into the main part of the flow by strong eddies, which are upwelling on the water surface as boils. The existence of these eddies causes the high concentration of suspended sediment.

(6) Measurements of instantaneous velocity fluctuations using a sonic current meter confirmed the existence of eddy motion. It is the variation of upward fluctuation of turbulent flow that agrees well with the spatial distribution of suspended sediment concentration.

The conclusion is as follows:

The flume experiments for unsteady flow make it clear that the dune development has a strong influence on turbulent flow structure and thus on sediment suspension. The results provide a plausible answer to the question why suspended sediment concentrations are higher during the rising stage of a flood in sand-bed rivers. Namely, the developing dune stage would be always present in the rising leg of a flood hydrograph. The dune development has a marked effect on sediment suspension in such rivers that the water discharge increases very rapidly.

ACKNOWLEDGEMENTS

The author expresses her appreciation to Professor Masao Inokuchi at the Institute of Geoscience of the University of Tsukuba for many helpful suggestions and encouragements. Flume experiments were carried out under the guidance of Lecturer Hiroshi Ikeda at the Environmental Research Center of the University of Tsukuba. Valuable discussions with Dr. Hiroshi Ikeda are gratefully acknowledged. Thanks are due to Dr. Kenji Kai at the Environmental Research Center for kind advice in preparing the computer program. The computations were performed by use of a FACOM M-200 computer at the Science Information Processing Center of the University of Tsukuba. Thanks are also due to Mr. Toyomori Kojima at the Environmental Research Center for making useful equipments, to Mr. Hideo Iijima at the Environmental Research Center and some students of the University of Tsukuba for their help in performing the measurement in flume, and to Dr. Shunji Oouchi for critical reading of this paper. The author wishes to express her sincere thanks to all persons who participated in the planning and the construction of the facility used in this experiment, and to Professor Masatoshi M. Yoshino, Director of the Environmental Research Center, for kind permission to publish this manuscript.

REFERENCES

Allen, J. R. L., 1976a, Computational models for dune time-lag: general ideas, difficulties and early results: *Sed. Geol.*, **15**, 1-53.

Allen, J. R. L., 1976b, Computational models for dune time-lag: population structures and the effects of discharge pattern and coefficient of change: *Sed. Geol.*, **16**, 99-130.

Allen, J. R. L., 1976c, Computational models for dune time-lag: an alternative boundary condition: *Sed. Geol.*, **16**, 255-279.

Allen, J. R. L., 1978, Computational models for dune time-lag: calculations using Stein's rule for dune height: *Sed. Geol.*, **20**, 165-216.

Allen, J. R. L., 1983, River bedforms: progress and problems: in Collison, J. D. and Lewin, J. ed., *Modern and Ancient Fluvial Systems, Spec. Publes Int. Ass. Sediment.*, **6**, University Press, Cambridge, 19-33.

Bagnold, R. A., 1966, An approach to the sediment transport problem from general physics: *U. S. Geol. Survey Prof. Paper*, **422-I**, 37p.

Coleman, J. M., 1969, Brahmaputra River: channel process and sedimentation: *Sed. Geol.*, **3**, 129-239.

Costello, W. R. and Southard, J. B., 1981, Flume experiments on lower-flow regime bed forms in coarse sand: *Jour. Sed. Petrology*, **51**, 849-864.

Einstein, H. A., Anderson, A. G. and Johnson, J. W., 1940, A distribution between bed load and suspended load in natural rivers: *Trans. Am. Geophys. Union*, **21**, II, 628-633.

Einstein, H. A., 1950, The bed-load function for sediment transportation in open channel flows: *U. S. Dept. Agriculture Soil Conservation Service Tech. Bull.*, **1026**, 78p.

Fredsøe, J., 1979, Unsteady flow in straight alluvial streams; modification of individual dunes: *Jour. Fluid, Mech.*, **91**, 497-512.

Fredsøe, J. 1981, Unsteady flow in straight alluvial streams. Part 2. Transition from dunes to plane bed: *Jour. Fluid Mech.*, **102**, 431-453.

Gibbs, R. J., 1974, A settling tube system for sand-size analysis: *Jour. Sed. Petrology*, **44**, 583-588.

Graf, W. H., 1971, *Hydraulics of sediment transport*: McGraw-Hill, New York, 513p.

Gregory, K. J. and Walling, D. E., 1973, *Drainage Basin Form and Process; A geomorphological approach*: Edward Arnold, London, 456p.

Guy, H. P., 1964, An analysis of some storm-period variables affecting stream sediment transport: *U. S. Geol. Survey Prof. Paper*, **462-E**, 45p.

Guy, H. P., Simons, D. B., and Richardson, E. B., 1966, Summary of alluvial channel data from flume experiments, 1956-61: *U. S. Geol. Survey Prof. Paper*, **462-I**, 96p.

Hall, D. G., 1967, The pattern of sediment movement in the River Tyne: *Internat. Assoc. Sci. Hyd. Pub.*, **75**, 117-142.

Heidel, S. G., 1956, The progressive lag of sediment concentration with flood waves: *Trans. Am. Geophys. Union*, **37**, 56-66.

Ikeda, H., 1983, Experiments on bedload transport, bed forms, and sedimentary structures using fine gravel in the 4-meter-wide flume: *Environ. Res. Center Papers*, Univ. of Tsukuba, **2**, 78p.

Ikeda, H. and Iseya, F., 1980, On the length of dunes in the lower Teshio River: *Trans. Japanese Geomor. Union*, **2**, 231-238.

Inokuchi, M., Ikeda, H., Izumi, K., Ono, Y. and Kawamata, R., 1980, The 4-meter wide flume in the Environmental Research Center: *Bull. Environ. Res. Center*, Univ. of Tsukuba, **4**, 55-87 (in Japanese).

Iseya, F., 1979, Suspended load and its sedimentation on the river side in the Sakura, Ibaraki Prefecture: *Proc. Japanese Conf. Hydraulics*, **23**, 145-150 (in Japanese).

Iseya, F., 1982a, A depositional process of reverse graded bedding in flood deposits of the Sakura River, Ibaraki Prefecture, Japan: *Geogr. Review Japan*, **55**, 597-613 (in Japanese with English abstract).

Iseya, F., 1982b, Suspended sediment in the Futagami River: *Bull. Environ. Res. Center*, Univ. of Tsukuba, **6**, 15-24 (in Japanese).

Jackson, R. G., 1976, Sedimentological and fluid-dynamic implications of the turbulent bursting phenomenon in geophysical flows: *Jour. Fluid Mech.*, **77**, 531-560.

Kai, K., 1982, Statistical characteristics of turbulence and the budget of turbulent energy in the surface boundary layer: *Environ. Res. Center Papers*, Univ. of Tsukuba, **1**, 54p.

Kennedy, J. F., 1963, The mechanics of dunes and antidunes in erodible-bed channels: *Jour. Fluid Mech.*, **16**, 521-544.

Kikkawa, H., 1954, Study on the changes of suspended load discharge during floods: *Rep. Public Works Res. Inst.*, Ministry of Construction, 97-101 (in Japanese).

Kikkawa, H. and Fukuoka, S., 1968, Hydraulic roles of wash load: *Trans. Japan Soc. Civil Engineers*, **155**, 42-52.

Kinoshita, R., 1982, Study of the flood deposits in the lower Ishikari River: Unpublished Rept. Civil Engineering Res. Inst., Hokkaido Development Bureau, 38p. (in Japanese).

Kline, S. J., Reynolds, W. C., Sohraub, F. A. and Rundstadler, P. W., 1967, The structure of turbulent boundary layer: *Jour. Fluid Mech.*, **30**, 741-773.

Korchokha, Yu. M., 1968, Investigation of the dune movement of sediments on the Polomet' River: *Sov. Hydrol.*, **161**, 541-559.

Lane, E. W. and Kalinske, A. A., 1939, The relation of suspended to bed material in rivers: *Trans. Am. Geophys. Union*, **20**, 637-641.

Leeder, M. R., 1983, On the interactions between turbulent flow, sediment transport and bedform mechanics in channelized flows: in Collinson, J. D. and Lewin, J. ed., *Modern and Ancient Fluvial Systems, Spec. Publs Int. Ass. Sediment.*, **6**, University Press, Cambridge, 5-18.

Leopold, L. B. and Maddock, T., 1953, The hydraulic geometry of stream channels and some physiographic implications: *U. S. Geol. Survey Prof. Paper*, **252**, 56p.

Lewin, J., 1983, River channel: in Goudie, A. ed., *Geomorphological Techniques*, George Allen & Union, London, 196-212.

Matthes, G. H., 1947, Macroturbulence in natural stream flow: *Trans. Am. Geophys. Union*, **28**, 255-262.

Mezaki, S., 1973, Bed forms in the Yoro River at Azu, Chiba Prefecture: *Geogr. Review Japan*, **46**, 516-532 (in Japanese with English abstract).

Middleton, G. V. and Southard, J. B., 1978, Mechanics of sediment movement: *Soc. Econ. Paleont. Miner. Short Course*, **3**, 246p.

Nordin, C. F., 1964, Aspects of flow resistance and sediment transport, Rio Grande near Bernalillo, New Mexico: *U. S. Geol. Survey Water-Supply Paper*, **1498-H**, 41p.

Nordin, C. F. and Beverage, J. P., 1965, Sediment transport in the Rio Grande, New Mexico: *U. S. Geol. Survey Prof. Paper*, **462F**, 35p.

Nordin, C. F. and Dempster, G. R., 1963, Vertical distribution of velocity and suspended sediment, middle Rio Grande, New Mexico: *U. S. Geol. Survey Prof. Paper*, **462-B**, 19p.

Nychas, S. G., Hershey, H. C. and Brodkey, R. S., 1973, A visual study of turbulent shear flow: *Jour. Fluid Mech.*, **61**, 513-540.

Offen, G. R. and Kline, S. J., 1975, A proposed model of the bursting process in turbulent boundary layers: *Jour. Fluid Mech.*, **70**, 209-228.

Raudkivi, A. J., 1967, *Loose Boundary Hydraulics*: Pergamon Press, Oxford, 331p.

Richard, K., 1982, *Rivers: form and process in alluvial channels*: Methuen, London, 358p.

Rouse, H., 1937, Modern conceptions of the mechanics of turbulence: *Trans. Am. Soc. Civil Engineers*, **102**, 463-505.

Scott, C. H. and Stephens, D., 1966, Special sediment investigations Mississippi River at St. Louis, Missouri, 1961-63: *U. S. Geol. Survey Water-Supply Paper*, **1819-J**, 43p.

Shen, H. W., 1971a, Total sediment: in Shen, H. W. ed., *River Mechanics*, Fort Collins, Colorado, 13-1–13-26.

Shen, H. W., 1971b, Wash load and bed load: in Shen, H. W. ed., *River Mechanics*, Fort Collins, Colorado, 11-1–11-30.

Simons, D. B. and Richardson, E. V., 1962, The effect of bed roughness on depth-discharge relations in alluvial channels: *U. S. Geol. Survey Water-Supply Irrig. Paper*, **1498-E**, 26p.

Simons, D. B., Richardson, E. V., and Nordrin, C. F., 1965, Sedimentary structures generated by flow in alluvial channels: in Middleton, G. V. ed., *Primary Sedimentary Structures and their Hydrodynamic Interpretation, Spec. Publs Soc. Econ. Paleont. Miner.*, Tulsa, **12**, 315-335.

Southard, J. B., 1971, Representation of bed configuration in depth- velocity-size diagrams: *Jour. Sed. Petrology*, **41**, 903-915.

Straub, L. G., 1932, Hydraulic and sedimentary characteristics of rivers: *Trans. Am. Geophys. Union*, **13**, 375-382.

Takagi, J, Makino, S., Takemoto, S. and Morita, Y., 1982, Field survey of flood flow and bed evolution in the lower Ishikari River: *Proc. Japanese Conf. Hydraulics*, **26**, 57-62 (in Japanese).

Tsuchiya, A., 1971, Flow resistance and bed forms in alluvial streams: *Proc. Annual Conf. Japan Soc. Civil Engineers*, **26**, II, 15-18 (in Japanese).

Vanoni, V. A., 1944, Transportation of suspended sediment by water: *Trans. Am. Soc. Civil Engineers*, **2267**, 67-102.

Vanoni, V. A., 1975, River Dynamics: in Yih, C. S. ed., *Advances in Applied Mechanics*, Academic Press, New York, 1-87.

Walling, D. E. and Teed, A., 1971, A simple pumping samplers for research into suspended sediment transport in small catchments: *Jour. Hydrology*, **13**, 325-337.

Wood, P. A., 1971, Controls of variation in suspended sediment concentration in the River Rother, West Sussex, England: *Sedimentology*, **24**, 437-445.

Yalin, M. S., 1972, *Mechanics of Sediment Transport*: Pergamon Press, Oxford, 290p.

APPENDIX A

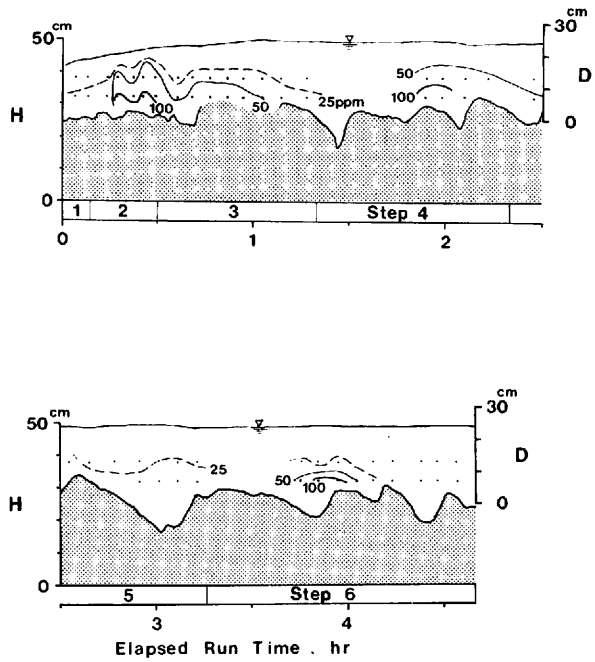

Fig. 25 Isopleths of suspended sediment concentration and the changes both of sand surface elevation and of water surface level at the sediment sampling point (Run 2). The upper figure is in the developing dune stage. The lower figure is in the equilibrium dune stage. D : mean water depth, H : height above the datum level

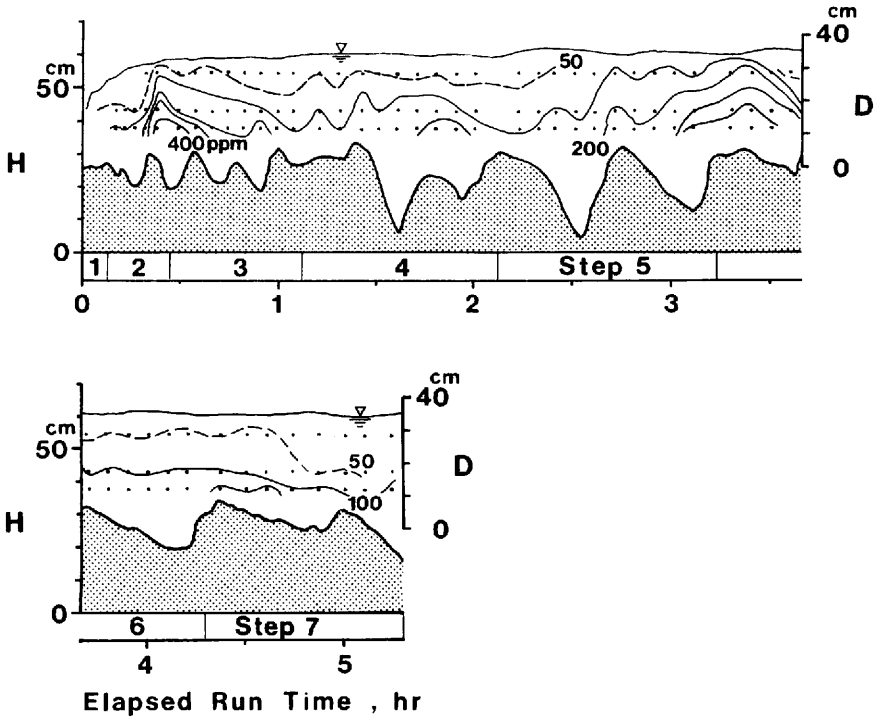

Fig. 26 Isopleths of suspended sediment concentration and the changes both of sand surface elevation and of water surface level at the sediment sampling point (Run 3). The upper figure is in the developing dune stage. The lower figure is in the equilibrium dune stage.
D : mean water depth, H : height above the datum level

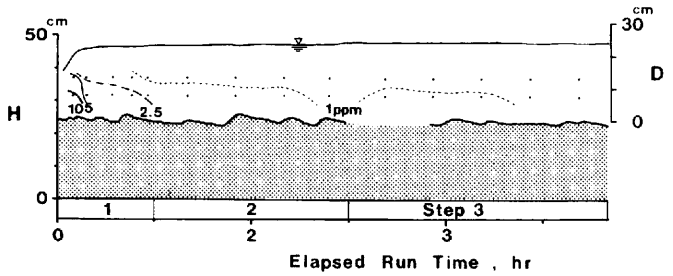

Fig. 27 Isopleths of suspended sediment concentration and the changes both of sand surface elevation and of water surface level at the sediment sampling point (Run 5).
D : mean water depth, H : height above the datum level

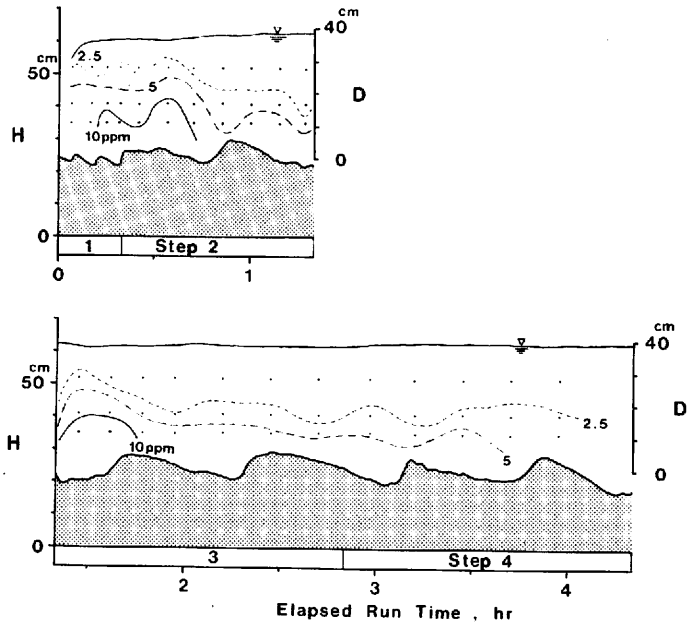

Fig. 28 Isopleths of suspended sediment concentration and the changes both of sand surface elevation and of water surface level at the sediment sampling point (Run 6). The upper figure is in the developing dune stage. The lower figure is in the equilibrium dune stage.

D : mean water depth, H : height above the datum level

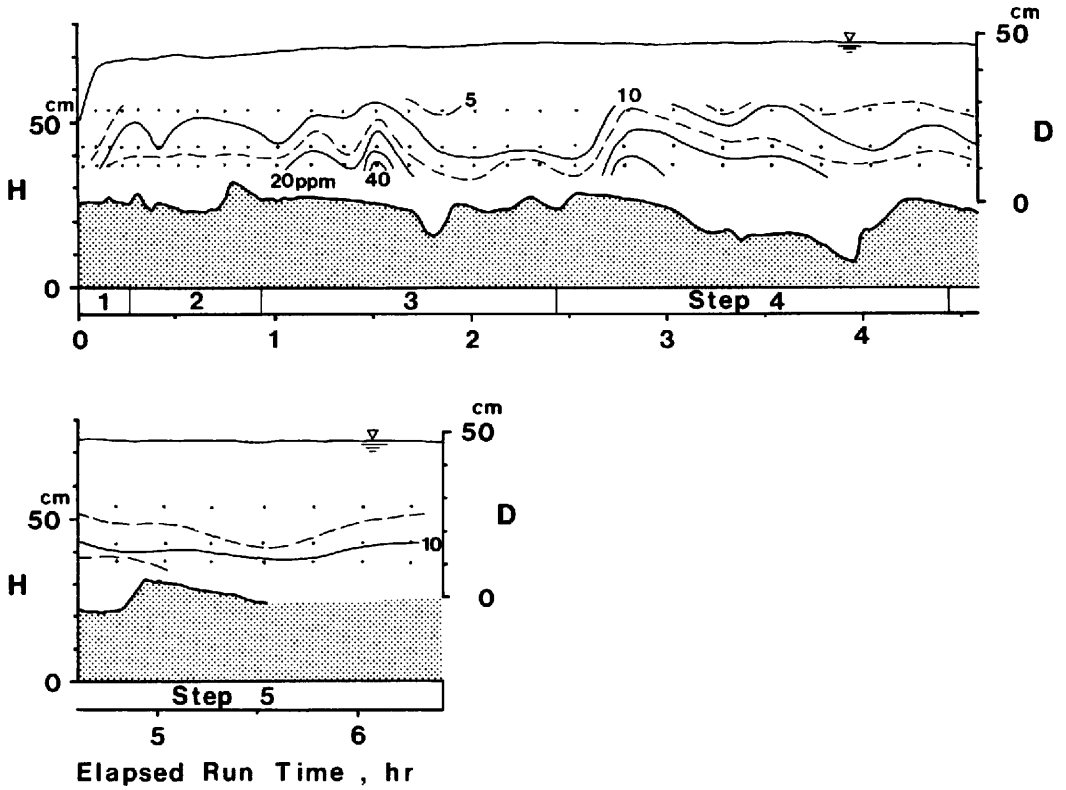

Fig. 29 Isopleths of suspended sediment concentration and the changes both of sand surface elevation and of water surface level at the sediment sampling point (Run 7). The upper figure is in the developing dune stage. The lower figure is in the equilibrium dune stage.
D : mean water depth, H : height above the datum level

APPENDIX B

Table 9 Data of suspended sediment concentration (Case 1)

RISING STAGE C_W = 105 ppm

T (min)	3	7	14	22	30	35	40	46	52	57	60	64
U (ppm)	–	–	–	–	–	–	–	–	–	–	–	–
M (ppm)	–	–	–	–	–	10.7	7.80	18.1	5.21	39.5	46.9	131
L (ppm)	17.9	4.70	17.8	12.7	12.8	43.7	23.4	58.6	37.5	170	224	205

T (min)	68	74	78	83	89	94	105	111	117	124	129
U (ppm)	–	–	–	32.1	65.6	156	175	129	95.7	106	69.3
M (ppm)	256	155	192	66.9	111	352	380	322	245	166	109
L (ppm)	345	320	390	123	229	483	–	–	–	–	–

FALLING STAGE C_W = 112 ppm

T (min)	142	149	154	160	176	182	188	194	200	211	216	223	230
U (ppm)	27.1	55.1	47.7	34.0	40.9	20.5	20.4	14.7	17.8	23.8	20.6	19.5	8.9
M (ppm)	39.5	77.2	107	74.0	70.6	55.1	32.3	31.7	48.3	65.6	43.4	35.1	22.9
L (ppm)	53.0	371	–	–	–	–	–	–	–	114	73.9	97.6	173

T (min)	238	247	257	268	278	291	297	306	316	324	337
U (ppm)	4.66	5.67	2.76	–	–	–	–	–	–	–	–
M (ppm)	10.8	46.5	10.2	5.64	13.9	17.4	6.74	7.57	7.28	3.20	2.15
L (ppm)	19.6	183	15.9	8.18	18.0	32.9	7.84	8.25	11.8	5.72	3.71

C_W: averaged wash load concentration, T: elapsed run time, L, M, U: lowermost, middle and uppermost sampling depth respectively

Table 10 Data of suspended sediment concentration (Run 2). For symbols, see Table 9.

STEP 1 C_W = 56.5 ppm

T (min)	3	8	14	17	22	25	29
M (ppm)	8.81	7.81	23.5	51.1	20.2	67.9	45.9
L (ppm)	37.1	44.3	44.2	101	69.3	115	56.8

STEP 2

T (min)	36	40.5	46	51.5	56.5	62.5	67.5	76.5
M (ppm)	20.3	30.0	33.7	24.8	29.8	28.9	19.0	14.1
L (ppm)	36.2	55.2	159	70.4	100	49.4	42.2	39.8

STEP 3

T (min)	113.5	117.5	125.5	133
M (ppm)	77.4	66.1	58.7	52.2
L (ppm)	169	176	449	–

STEP 4 C_W = 62.3 ppm

T (min)	147	153	159	167	175	181	187	193
M (ppm)	34.7	36.4	14.0	14.6	19.5	25.5	29.8	10.8
L (ppm)	59.2	95.9	98.7	–	36.2	32.3	55.5	40.6

STEP 5

T (min)	225.5	231	237	254	263	268	273
M (ppm)	28.7	12.2	30.8	8.12	14.9	13.3	11.1
L (ppm)	52.7	182	165	–	16.1	21.6	33.9

Table 11 Data of suspended sediment concentration (Run 3). For symbols, see Table 9.

STEP 2

T (min)	10.5	13	16	19.5	23
U (ppm)	–	–	–	11.8	95.9
M (ppm)	64.8	56.6	47.2	63.3	355
L (ppm)	105	96.0	94.7	210	419

STEP 3 C_W = 78.2 ppm

T (min)	29.5	34.5	39.5	44.5	49.5	54.5	59.5	64.5
U (ppm)	38.7	52.1	69.6	38.5	33.6	37.4	35.0	28.3
M (ppm)	157	161	150	106	141	108	86.4	71.8
L (ppm)	412	318	203	162	248	273	128	97.5

STEP 4 C_W = 86.4 ppm

T (min)	72.5	79	85.5	90.5	96.5	102.5	108.5	114.5	120.5
U (ppm)	48.8	34.4	66.1	49.6	59.6	58.5	49.8	27.0	40.4
M (ppm)	109	79.1	137	104	120	128	168	116	82.9
L (ppm)	115	99.9	181	144	156	181	260	259	138

STEP 5

T (min)	134	140	145	151	157	163	169	175	181	187
U (ppm)	30.0	44.6	55.5	63.2	85.0	110	85.8	104	112	93.5
M (ppm)	60.8	91.2	112	94.0	171	211	145	182	234	307
L (ppm)	74.6	108	127	108	173	219	214	191	273	446

STEP 6

T (min)	198.5	204.5	210.5	216.5	221.5	228.5	234.5	240.5	246.5	252.5
U (ppm)	198	227	101	39.3	41.1	51.2	38.3	43.4	58.2	57.3
M (ppm)	358	422	303	293	91.1	128	88.6	86.5	106	109
L (ppm)	456	579	451	–	165	163	117	114	124	128

STEP 7 C_W = 90.3 ppm

T (min)	262.5	270.5	276.5	284.5	292.5	300.5	307.5	315.5
U (ppm)	49.6	62.7	89.7	20.5	18.3	20.7	15.4	15.5
M (ppm)	106	128	189	63.4	48.3	55.0	39.9	35.0
L (ppm)	227	196	269	100	111	74.6	54.8	42.2

Table 12 Data of suspended sediment concentration (Run 4). For symbols, see Table 9.

STEP 1 C_w = 87.7 ppm

T (min)	1	2	3
U (ppm)	–	–	–
M (ppm)	–	–	–
L (ppm)	97.4	132	90.3

STEP 2 C_w = 90.3 ppm

T (min)	4	5	6	7
U (ppm)	–	–	–	–
M (ppm)	–	–	–	–
L (ppm)	294	218	172	174

STEP 3 C_w = 91.5 ppm

T (min)	9	10	11	12	13.5	15	16.5	18	19	21
U (ppm)	–	–	–	–	–	–	–	–	–	–
M (ppm)	–	–	–	–	–	–	–	–	–	–
L (ppm)	154	468	408	297	303	394	371	487	591	368

STEP 4 C_w = 92.5 ppm

T (min)	27.5	33	36.5	41	44	50
U (ppm)	118	123	115	161	155	105
M (ppm)	212	201	229	334	319	194
L (ppm)	245	505	340	456	400	281

STEP 5 C_w = 90.7 ppm

T (min)	66	72	75	81	85	97	102	107	112	117	141	146	151
U (ppm)	158	273	286	120	86.3	79.6	169	199	153	102	158	319	60.5
M (ppm)	229	461	699	279	156	135	372	331	259	175	239	445	121
L (ppm)	270	583	1100	465	287	173	496	445	338	232	296	558	167

T (min)	156	160
U (ppm)	127	226
M (ppm)	236	403
L (ppm)	331	555

STEP 6 C_W = 88.5 ppm

T (min)	181	187	193	199	207	213	219	225	231	237	243	249	256
U (ppm)	146	244	113	159	108	66.5	92.1	46.3	29.5	33.5	80.4	77.9	106
M (ppm)	432	376	238	368	239	116	153	99.3	57.3	62.8	122	127	169
L (ppm)	911	–	–	–	–	–	202	129	75.1	99.3	196	174	207

T (min)	261	267	273	279	285	290
U (ppm)	79.8	90.2	133	198	183	115
M (ppm)	143	170	233	301	260	190
L (ppm)	174	213	284	341	290	208

STEP 7 C_W = 90.8 ppm

T (min)	296	301	307	313	319	325	331	337	343	349	355	361	367
U (ppm)	89.9	48.5	153	129	99.7	104	73.6	82.0	96.0	97.9	92.0	99.9	82.8
M (ppm)	136	133	215	181	151	160	138	144	139	174	142	163	148
L (ppm)	165	170	234	236	190	208	199	189	167	243	168	193	171

T (min)	373	379	385	391	397	403	409
U (ppm)	82.2	97.8	96.0	96.4	119	86.9	102
M (ppm)	147	169	166	156	178	139	146
L (ppm)	171	216	200	184	207	173	176

STEP 8 C_W = 85.9 ppm

T (min)	419	425	431	437	443	449	456	461	467	473	479	485	491
U (ppm)	53.2	81.7	94.8	73.7	55.7	43.6	38.1	48.8	55.7	34.7	35.0	20.1	27.6
M (ppm)	84.8	126	162	115	85.8	64.8	62.9	83.7	95.2	115	66.9	42.6	51.7
L (ppm)	103	153	205	134	90.4	81.9	76.6	103	124	371	93.0	61.7	66.9

T (min)	497	503	509	515	521	527
U (ppm)	36.1	34.3	54.9	30.3	56.8	82.1
M (ppm)	60.4	54.6	79.8	59.6	104	138
L (ppm)	75.3	88.9	96.2	74.5	127	173

Table 13 Data of suspended sediment concentration (Run 5). For symbols, see Table 9.

STEP 1 C_W = 50.3 ppm

T (min)	5	9	17	23	28
M (ppm)	6.02	1.89	2.22	1.55	0.625
L (ppm)	10.4	3.91	3.36	3.63	2.42

STEP 2

T (min)	40	55	70	84
M (ppm)	0.852	0.646	0.671	0.416
L (ppm)	2.12	1.56	1.40	0.656

STEP 3 C_W = 58.1 ppm

T (min)	101	116	131	146	151
M (ppm)	0.654	0.649	0.662	0.129	0.507
L (ppm)	1.62	1.22	1.27	0.374	0.736

Table 14 Data of suspended sediment concentration (Run 6). For symbols, see Table 9.

STEP 1

T (min)	4	10	15	19
U (ppm)	2.61	1.62	1.85	2.72
M (ppm)	7.04	5.38	6.98	5.45
L (ppm)	8.80	6.57	24.5	10.8

STEP 2

T (min)	25	34	42	51	60	69	77
U (ppm)	2.20	3.55	2.26	0.925	1.06	1.28	0.652
M (ppm)	5.24	11.3	6.64	2.82	3.53	2.69	1.29
L (ppm)	8.02	24.9	9.64	4.21	6.99	6.74	3.30

STEP 3 C_W = 59.0 ppm

T (min)	87	97	107	117	132	147	162
U (ppm)	2.21	1.42	1.37	0.924	1.29	0.945	0.957
M (ppm)	7.76	9.51	4.06	2.52	3.16	2.87	1.58
L (ppm)	23.1	16.9	5.99	6.69	7.97	5.78	4.39

STEP 4 C_W = 61.6 ppm

T (min)	178	192	207	222	237
U (ppm)	0.950	0.702	1.01	1.64	0.605
M (ppm)	3.25	1.82	3.26	3.04	2.76
L (ppm)	4.95	4.05	6.55	3.92	4.15

Table 15 Data of suspended sediment concentration (Run 7). For symbols, see Table 9.

STEP 1

T (min)	6	10	14
U (ppm)	3.97	4.57	8.28
M (ppm)	3.41	9.87	11.8
L (ppm)	7.03	15.0	–

STEP 2 C_W = 69.8 ppm

T (min)	19	25	31	37	45	52
U (ppm)	7.17	6.18	6.20	9.27	7.33	7.53
M (ppm)	12.4	9.50	13.3	11.9	12.7	11.4
L (ppm)	16.2	12.5	19.8	16.2	19.6	17.6

STEP 3

T (min)	61	71	81	91	101	111	121	131	141
U (ppm)	5.84	9.38	7.47	13.4	6.41	5.34	4.16	4.59	4.84
M (ppm)	10.7	18.6	13.4	26.0	11.3	9.04	8.11	9.29	9.17
L (ppm)	15.9	28.8	19.6	42.6	16.8	13.0	12.9	16.6	15.9

STEP 4

T (min)	152	167	182	197	212	227	242	257
U (ppm)	3.95	15.3	11.6	6.88	11.8	4.05	5.17	5.52
M (ppm)	7.71	23.5	21.7	16.8	15.9	11.8	9.65	14.3
L (ppm)	10.9	33.7	23.0	21.0	24.5	18.8	15.2	20.7

STEP 5 C_W = 72.5 ppm

T (min)	272	287	302	316	332	347	361	376
U (ppm)	4.56	4.03	3.60	2.71	2.31	3.05	3.12	4.11
M (ppm)	11.6	7.30	8.35	6.83	4.52	5.58	9.12	10.2
L (ppm)	18.0	17.2	13.0	13.2	11.4	11.0	11.5	16.2

Environmental Research Center Papers

No. 1 (1982) Kenji KAI: Statistical characteristics of turbulence and the budget of turbulent energy in the surface boundary layer. 54p.

No. 2 (1983) Hiroshi IKEDA: Experiments on bedload transport, bed forms, and sedimentary structures using fine gravel in the 4-meter-wide flume. 78p.

No. 3 (1983) Yousay HAYASHI: Aerodynamical properties of an air layer affected by vegetation. 54p.

No. 4 (1984) Shinji NAKAGAWA: Study on evapotranspiration from pasture. 87p.

No. 5 (1984) Fujiko ISEYA: An experimental study of dune development and its effect on sediment suspension. 56p.

発行　　昭和59年3月25日

編集・発行者　筑波大学水理実験センター

〒305 茨城県新治郡桜村天王台1－1－1

TEL 0298(53)2532, 2534

印刷　日青工業株式会社

東京都港区西新橋2－5－10